

Shape constrained kernel-weighted least squares:

Application to production function estimation for Chilean manufacturing industries

Daisuke Yagi^a, Andrew L. Johnson^a and Timo Kuosmanen^b

Abstract

Two approaches to nonparametric regression include local averaging and shape constrained regression. In this paper we examine a novel way to impose shape constraints on a local linear kernel estimator. The proposed approach is referred to as Shape Constrained Kernel-weighted Least Squares (SCKLS). We prove consistency of SCKLS estimator and show that SCKLS is a generalization of Convex Nonparametric Least Squares (CNLS). We compare the performance of three estimators, SCKLS, CNLS, and Constrained Weighted Bootstrap, via Monte Carlo simulations. From the simulation results, we conclude that SCKLS performance is very competitive and provides better out-of-sample prediction than existing estimators. We analyze Chilean manufacturing data using the SCKLS estimator and quantify production in the plastics and wood industries. Importantly we find firms that export have significantly higher productivity.

JEL Codes: C14, D24

Keywords: *Kernel Estimation, Multivariate Convex Regression, Nonparametric regression, Shape Constraints.*

^aDepartment of Industrial and Systems Engineering, Texas A&M University, TX, USA

^bSchool of Business, Aalto University, Helsinki, Finland

1. Introduction

Nonparametric methods avoid functional form misspecification, but suffer from the curse of dimensionality. For modeling production with a production or a cost function, the extremely flexible nature of nonparametric methods often cause difficulties in interpreting the results. However, microeconomic theory provides additional structure for modeling production which can be stated as shape constraints. Recently several nonparametric shape constrained estimators have been proposed that combine the advantage of avoiding parametric functional specification with improved small sample performance relative to unconstrained nonparametric estimators. However, the existing methods tend to either overfit the observed sample causing poor out-of-sample prediction or have computational issues. We propose an estimator that impose shape restrictions on local kernel weighting methods. By introducing local averaging, we improve small sample performance, but avoid the overfitting and computational challenges of existing shape constrained estimation methods.

Starting with the univariate regressor case, nonparametric regression with a least squares objective subject to monotonicity and concavity constraints was studied in the 1950s, Hildreth (1954). See also Brunk (1955) and Grenander (1956) for alternative shape constrained estimators. Properties such as consistency, rate of convergence, and asymptotic distribution are shown by Hanson and Pledger (1976), Mammen (1991), and Groeneboom et al. (2001), respectively. Holloway (1979) experiment with multiple predictor variables and Banker and Maindiratta (1992) proposed a maximum likelihood formulation and Sarath and Maindiratta (1997) prove its consistency. The multivariate characterization and consistency of least squares estimator, which we will refer to as Convex Nonparametric Least Squares (CNLS), is shown by Kuosmanen (2008) and Seijo and Sen (2011), respectively.

Regarding the nonparametric estimation implemented using kernel based methods, Birke and Dette (2007), Carroll et al. (2011), and Hall and Huang (2001) investigated the univariate case and proposed a smooth estimator that can impose derivative-based constraints including monotonicity and concavity/convexity. Du et al. (2013) proposed Constrained Weighted Bootstrap (CWB) by generalizing Hall and Huang's method to the multivariate regressors setting. However, CWB still faces significant computational difficulties.

In this paper, we propose a new estimator called Shape Constrained Kernel-weighted Least Squares (SCKLS) which optimizes a local linear kernel criterion while estimating a multivariate regression function with shape constraints. We prove consistency of SCKLS estimator and show that the SCKLS estimator is equivalent to the CNLS estimator when the bandwidth of the kernel approaches zero. Kuosmanen (2008), Seijo and Sen (2011) and Lim and Glynn (2012) emphasize as one of the major advantages of CNLS that it does not have any tuning parameters such as bandwidth selection. The proposed SCKLS estimator sheds further light on this issue: in the SCKLS framework, CNLS can be seen as the zero bandwidth estimator. We also show that the SCKLS estimator is equivalent to linear regression subject to monotonicity constraints as the bandwidth approaches infinity.

Both CNLS and CWB impose $O(n^2)$ concavity/convexity constraints, which lead to computational difficulties. We propose an iterative algorithm to reduce the number of constraints building on the ideas in Lee et al. (2013). We validate the performance of the SCKLS estimator via Monte Carlo simulations. For a variety of parameter settings we find the performance of SCKLS to be better or at least very competitive with CNLS and CWB estimator. We also validate the usefulness of the iterative algorithm to reduce computational time through the simulations. We investigate the use of variable bandwidth methods and find that these methods lead to relatively

flat (very little curvature) functions. Thus, we propose an alternative of using a relatively small fixed bandwidth on an adjusted grid.

This paper will focus on production functions thus guiding the selection of the function for the data generation process in the Monte Carlo simulations and for the application analyzing the Chilean manufacturing data. Therefore, the primary shape constraints of interest are monotonicity and concavity. These assumptions are motivated from standard economic theory for consumer preferences and production functions (Varian, 1982, 1984). However, the methods proposed are general and applicable for other applications of shape restricted functional estimation.

We implement the SCKLS estimator empirically on Chilean manufacturing data from the Chilean Annual Industrial Survey. The estimation results provide a concise description of the supply-side of the Chilean plastic and wood industry as we report marginal productivity, marginal rate of substitution and most productive scale size. We also investigate the impact of exporting on the productivity by including additional predictors of output in a semi-parametric model. We find that exporting is correlated with higher productivity supporting international trade theories that argue high productivity firms are more likely to compete in international markets.

The remainder of this paper is as follows. Section 2 describes the existing estimators, CNLS and CWB. Section 3 presented the proposed estimator, SCKLS. Section 4 contains the proof of consistency of SCKLS estimator. Section 5 discusses the Monte Carlo simulation results for a set of three estimator (SCKLS, CNLS and CWB) under several different experimental settings. Section 6 applies the SCKLS estimator to estimate a production function for both the Chilean plastics and wood industries. Section 7 concludes and suggests future research directions. An on-line appendix discusses several extensions to the CWB estimator and describes the relationship

between SCKLS, CWB and CNLS. A more extensive set of results related to Experiments 1-4 are reported and details of the iterative algorithm for SCKLS is provided.

2. Model and Existing Estimators

The following section introduces the model and describes two existing nonparametric estimation methods with concavity/convexity and monotonicity constraints.

2.1. Model

Consider the following regression model

$$y = g_0(\mathbf{x}) + \varepsilon$$

where $\mathbf{x} \in \mathbf{X} \subset \mathbb{R}^d, d \geq 1$ is a vector of random variables of length d and $y \in \mathbb{R}$ is a random variable, and ε is a random variable satisfying $E(\varepsilon|\mathbf{x}) = 0$. The regression function $g_0(\cdot)$ is assumed to belong to a class of functions, G , that satisfy certain shape restrictions. Building on the structure proposed by Du et al. (2013) our estimator can impose any shape restriction that can be modelled as a lower or upper bound on a derivate. Examples are supermodularity, convexity, monotonicity, or quasi-convexity. For purposes of concreteness, we will focus on imposing monotonicity and convexity/concavity.

Thus, throughout this paper we will assume $g_0 \in G_2$ where G_2 is the set of all monotonic and convex/concave function. Specifically g_0 is convex if:

$$\lambda g_0(\mathbf{x}_1) + (1 - \lambda)g_0(\mathbf{x}_2) \geq g_0(\lambda\mathbf{x}_1 + (1 - \lambda)\mathbf{x}_2)$$

for every $\mathbf{x}_1, \mathbf{x}_2 \in \mathbf{X}$ and $\lambda \in [0, 1]$. Further monotonically increasing implies:

$$\text{If } \mathbf{x}_1 \leq \mathbf{x}_2, \text{ then } g_0(\mathbf{x}_1) \leq g_0(\mathbf{x}_2)$$

where \mathbf{x}_1 and \mathbf{x}_2 are vectors such that the inequality implies that every component of \mathbf{x}_2 is greater than or equal to every component of \mathbf{x}_1 .

2.2. Convex Nonparametric Least Squares (CNLS)

Kuosmanen (2008) extends Hildreth's least squares approach to the multivariate setting with a multivariate \mathbf{x} , and coins the term Convex Nonparametric Least Squares (CNLS). CNLS builds upon the assumption that the true but unknown production function g belongs to the set of continuous, monotonic increasing and globally concave functions, G_2 . Let $\{\mathbf{X}_j, y_j\}_{j=1}^n$ denote sample pairs of input and output data, where $\mathbf{X}_j = (X_{j1}, \dots, X_{jd})'$ is an input vector, and y_j is an output scalar. A set of unique fitted values, $\hat{y}_j = \hat{\alpha}_j + \hat{\boldsymbol{\beta}}_j' \mathbf{X}_j$, can be found by solving the quadratic programming (QP) problem

$$\begin{aligned} \min_{\alpha, \boldsymbol{\beta}} \sum_{j=1}^n \left(y_j - (\alpha_j + \boldsymbol{\beta}_j' \mathbf{X}_j) \right)^2 \\ \text{subject to} \\ \alpha_j + \boldsymbol{\beta}_j' \mathbf{X}_j \leq \alpha_l + \boldsymbol{\beta}_l' \mathbf{X}_j \quad j, l = 1, \dots, n \\ \boldsymbol{\beta}_j \geq 0 \quad j = 1, \dots, n \end{aligned} \tag{1}$$

where α_j and $\boldsymbol{\beta}_j$ define the intercept and slope parameters that characterize the estimated piece-wise hyperplane that are tangent to the true production function. The inequality constraints in (1) can be interpreted as a system of Afriat inequalities (Afriat 1972; Varian 1984) to impose concavity constraints. We emphasize that CNLS does not assume or restrict the domain G_2 to only include the piece-wise linear function or assume the smoothness of the function. Thus, the estimate

resulting from (1) is the most flexible¹ estimator that satisfies the shapes constraints and that the data supports. We also note that the functional estimates resulting from (1) is unique only for the observed data points.

2.3. Constrained Weighted Bootstrap (CWB)

Hall and Huang (2001) proposed the monotone kernel regression method in univariate function. Du et al. (2013) generalized this model to handle multiple general shape constraints for multivariate functions, which they refer to as Constrained Weighted Bootstrap (CWB). CWB estimator is constructed by introducing weights for each observed data point. The weights are selected to minimize the distance to unconstrained estimator while satisfying the shape constraints. The function is estimated as

$$\hat{g}(\mathbf{x}|\mathbf{p}) = \sum_{j=1}^n p_j A_j(\mathbf{x}) y_j \quad (2)$$

where p_i is the weights introduced for each observation and $A_i(\mathbf{x})$ is a local weighting matrix (e.g. local linear kernel weighting matrix). Du et al. (2013) relax the Hall and Huang (2001) restriction that p_i is non-negative and propose to calculate p_i by minimizing the distance to unrestricted weights, $p_u = 1/n$, under $\sum_{j=1}^n p_j = 1$ and derivative-based shape constraints. The problem is formulated as follows.

¹ Typically, “smooth” refers to the existence of a certain number of derivatives. The CNLS estimator has discontinuities in the derivative. Therefore, we use “more flexible” to refer to a function that is approximated with more rather than fewer hyperplanes.

$$\min_{\mathbf{p}} D(\mathbf{p}) = \sum_{j=1}^n (p_j - p_u)^2 = \sum_{j=1}^n \left(p_j - \frac{1}{n}\right)^2$$

subject to

$$l(\mathbf{x}_i) \leq \hat{g}^{(s)}(\mathbf{x}_i|\mathbf{p}) \leq u(\mathbf{x}_i) \quad i = 1, \dots, m \quad (3)$$

$$\sum_{j=1}^n p_j = 1$$

where \mathbf{x}_i represents a set of points for evaluating constraints and the elements of \mathbf{s} represent the order of partial derivative. Here we use the notation, $l(\mathbf{x})$ and $u(\mathbf{x})$, to emphasize that the bounds needed to impose restrictions on functional derivatives are typically functions of the entire data set \mathbf{x} . Specifically, the shape restrictions are imposed at a set of evaluation points $\{\mathbf{x}_i\}_{i=1}^m$. Further, $g^{(s)}(\mathbf{x}) = [\partial^{s_1} g(\mathbf{x}) \cdots \partial^{s_r} g(\mathbf{x})] / [\partial x_1^{s_1} \cdots \partial x_r^{s_r}]$ for $\mathbf{s} = (s_1, s_2, \dots, s_r)$. We can impose concavity/convexity and monotonicity constraints by setting appropriate lower bound $l(\mathbf{x})$ or upper bound $u(\mathbf{x})$ to the first partial derivative of the function. Although CWB estimator results in a smooth function, the estimated function only satisfies the shape restrictions locally around the evaluation points on which they are imposed.

One way to interpret the CWB estimator is as a two-step process: 1) estimate an unconstrained kernel estimator; 2) find the shape constrained function that is as close as possible (as measured by the Euclidean distance in \mathbf{p} -space) to the unconstrained kernel estimator. This estimator is conceptual simple; however, this procedure potentially pulls the functional estimate away from the data and towards the unrestricted estimate. Thus, the CWB estimator suffers from computational difficulties and poor estimates in small samples as demonstrated in Section 4.

Appendix A proposes changing the objective function to minimize the distance from the estimated function to the observed data, which seems to improve the estimates.²

3. Shape Constrained Kernel-weighted Least Squares (SCKLS)

The local linear kernel estimator developed by Stone (1977) and Cleveland (1979) is defined as

$$\min_{a, \mathbf{b}} \sum_{j=1}^n \left(y_j - a - (\mathbf{X}_j - \mathbf{x})' \mathbf{b} \right)^2 K \left(\frac{\mathbf{X}_j - \mathbf{x}}{\mathbf{h}} \right) \quad (4)$$

where a is a functional estimate, and \mathbf{b} is an estimate of the slope of the function at \mathbf{x} where \mathbf{x} is an arbitrary point in input space, $K \left(\frac{\mathbf{X}_j - \mathbf{x}}{\mathbf{h}} \right)$ denotes a product kernel, and \mathbf{h} is a vector of the bandwidth (see Racine and Li (2004)). The objective function uses kernel weights, so more weight is given to the observations that are closer to the evaluation point \mathbf{x} .

We introduce a set of points for evaluating constraints, which we call evaluation points, and impose shape constraints on the local linear kernel estimator. In the spirit of local linear kernel estimator, we define Shape Constrained Kernel-weighted Least Squares (SCKLS) estimator as

$$\begin{aligned} & \min_{a_i, \mathbf{b}_i} \sum_{i=1}^m \sum_{j=1}^n \left(y_j - a_i - (\mathbf{X}_j - \mathbf{x}_i)' \mathbf{b}_i \right)^2 K \left(\frac{\mathbf{X}_j - \mathbf{x}_i}{\mathbf{h}} \right) \\ & \text{subject to} \\ & l(\mathbf{x}_i) \leq \hat{g}^{(s)}(\mathbf{x}_i | \mathbf{a}, \mathbf{b}) \leq u(\mathbf{x}_i) \quad i = 1, \dots, m \end{aligned} \quad (5)$$

For the case of monotonicity and concavity, these constraints can be written explicitly as

² We refer to the estimator that minimizes the distance from the estimated function to the observed data as the CWB in y-space, and to the original CWB estimator as CWB in p-space, respectively. Appendix D presents a comparison of these estimators.

$$\min_{\mathbf{a}, \mathbf{b}_i} \sum_{i=1}^m \sum_{j=1}^n \left(y_j - a_i - (\mathbf{X}_j - \mathbf{x}_i)' \mathbf{b}_i \right)^2 K \left(\frac{\mathbf{X}_j - \mathbf{x}_i}{\mathbf{h}} \right)$$

subject to

$$a_i - a_l \geq \mathbf{b}_i'(x_i - x_l) \quad i, l = 1, \dots, m$$

$$b_i \geq 0 \quad i = 1, \dots, m$$
(6)

The first set of constraints in (6) imposes concavity and the second set of constraints imposes non-negativity of \mathbf{b}_i at each evaluation point $\{\mathbf{x}_i\}_{i=1}^m$ where m denotes the number of evaluation points.

From the results of (6) define the SKLS estimator to be the function $\hat{g}_n: \mathbb{R}^d \rightarrow \mathbb{R}$ defined by

$$\hat{g}_n(x; \mathbf{a}, \mathbf{b}) = \min_{i \in \{1, \dots, m\}} a_i - (\mathbf{x}_i)' \mathbf{b}_i$$

For any $\mathbf{x} \in \mathbb{R}^d$.

A standard method for determining \mathbf{x}_i is to construct a uniform grid. As the density of \mathbf{x}_i increases, the estimated function potentially has more hyperplanes and is more flexible; however, the computation time increases. If a smooth functional estimate is preferred, Nesterov (2005) and Mazumder (2015) provide methods for this smoothing.³

Figure 1 illustrates the relationship between the SCKLS, CNLS and CWB estimators. The gray area indicates the cone of concave and monotonic functions. CNLS estimates a monotonic and concave function while minimizing the sum of squared errors, that is, minimizing the distance from the origin to the cone in ϵ -space. CWB estimates a monotonic and concave function by finding the closest point on the cone of concave and monotonic functions to unconstrained kernel estimate. SCKLS minimizes a weighted function of ϵ , and therefore avoids overfitting the

³ A piece-wise linear approximation is often believed to be a poor estimator for a smooth underlying function. Appendix B presents a limited comparison between shape constrained p-splines and SCKLS. The results indicate that, even the smooth p-splines estimator, the estimated function is often approximately piece-wise linear when the true function is monotonic and concave and the estimator is fit is a small set of data.

observed data, but also attempts to fit the data as closely as possible, rather than minimizing the distance from the unconstrained kernel estimator.

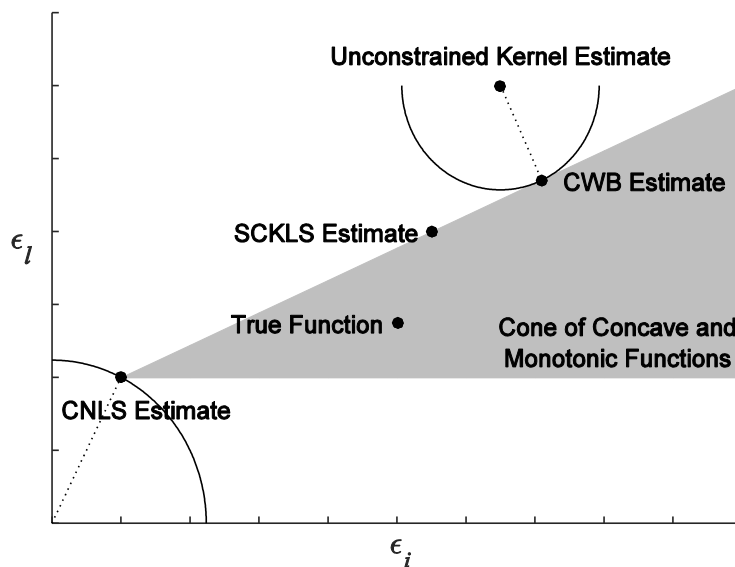


Figure 1. Comparison of each estimator in ϵ -space

Our primary application of interest is production functions estimated for census manufacturing data where the input distributions are often highly skewed meaning there are many small establishments, but relatively few large establishments.⁴ We propose two methods to address this issue. First, we propose to use a k-nearest neighbor (k-NN) approach for bandwidth selection in SKLS which we will refer to as SCKLS k-NN. k-NN approach uses a smaller bandwidth for smoothing in dense data regions and a larger bandwidth when the data is sparser. For a further description of the method see for example Li and Racine (2007). The formulation of SCKLS k-NN leads to a different weighting in the objective function.

⁴ An establishment is defined as a single physical location where business is conducted or where services or industrial operations are performed.

$$\min_{a_i, b_i} \sum_{i=1}^m \sum_{j=1}^n \left(y_j - a_i - (\mathbf{X}_j - \mathbf{x}_i)' \mathbf{b}_i \right)^2 w \left(\frac{\|\mathbf{X}_j - \mathbf{x}_i\|}{R_{x_i}} \right)$$

(7)

subject to

$$a_i - a_l \geq b_i'(x_i - x_l) \quad i, l = 1, \dots, m$$

$$b_i \geq 0 \quad i = 1, \dots, m$$

where $w(\cdot)$ is a general weight function, $\|\cdot\|$ is the Euclidian norm and R_{x_i} denotes the Euclidian distance between \mathbf{x}_i and k -th nearest neighbor of \mathbf{x}_i among $\{\mathbf{X}_j\}_{j=1}^n$.

For CWB and SCKLS estimator, we need to specify how to select the evaluation points before implementation. The standard method is a uniform grid where each dimension is divided into equal spaces. However, we can also address the skewness problem by constructing the evaluation points differently. Thus, our second method is to use a non-uniform grid method. We first use kernel density estimation to estimate the density function for each input dimension. Then we take the equally spaced percentiles of the estimated density function and construct non-uniform grid. Figure 2 demonstrates how the non-uniform grid are constructed for the 2-dimensional case. In this example, we set the minimum and maximum of the observed data as the edge of the grid, and compute equally spaced percentile. We discuss the impacts of these extensions in section 5 where the simulation results are presented.

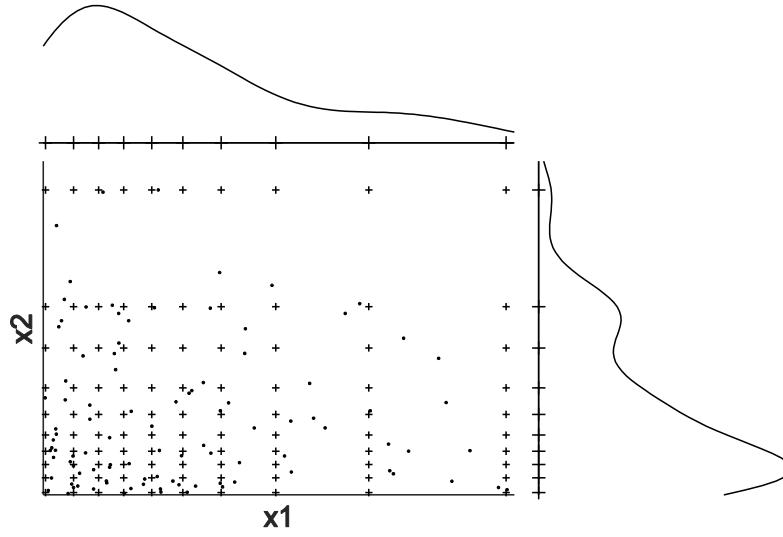


Figure 2. Example of non-uniform grid with kernel density estimation in 2-dimensional case

4. Properties of SCKLS

We next consider the statistical properties of the SCKLS estimator. We first prove the consistency of SCKLS. Further, we explain and prove the relationship between the SCKLS, CNLS, and sign constrained linear regression. First, we show the relationship between the CNLS estimator and the SCKLS estimator, specifically the case where the bandwidth in the SCKLS estimator approaches to zero, the estimates converge to the CNLS estimates. Second, we show that as the bandwidth in the SCKLS estimator approaches to infinity, the estimates converge to linear regression subject to monotonicity constraints.

4.1. Consistency of SCKLS

Let $g(\mathbf{x})$ denote the true unknown function and define the conditional mean as $E[y|\mathbf{x}]$ and g^D be the derivative of $g(\cdot)$. Further, let $f(\mathbf{x})$ be a probability density function of \mathbf{x} , and G_2 as the class of function which is continuous, monotonic increasing and globally concave functions.

Assumption 1.

- (i). $g \in G_2$.
- (ii). $\{X_j, y_j\}_{j=1}^n$ are i. i. d.
- (iii). $g(x), f(x)$ and $\sigma^2(x) = E[u_i^2 | x]$, are twice differentiable.
- (iv). The kernel function, $K(\cdot)$ is symmetric, compactly supported density such that K^D is Hölder-continuous on the domain of X .
- (v). The bandwidth associated with each explanatory variable, $h_j, h_j \propto n^{-1/(3r+2|\mathbf{d}|)}, 1 \leq j \leq r$, where $|\mathbf{d}|$ is the maximum order of the derivative vector \mathbf{d} .

Assumption 1 (i) states that the constraints we impose on the SCKLS estimator are satisfied by the true function. (ii) states the data is i.i.d and thus the residuals from an regression model estimated using this data are also i.i.d. (iii) assumes derivatives are defined for the function of interest. Finally (iv) and (v) assures the bandwidths become sufficiently small as $n \rightarrow \infty$ so averaging does not introduce bias. For details of the consistency of local linear estimator, see Li and Racine (2007).

Theorem 1. *Suppose that Assumption 1 (i) – (v) holds. Then*

$$\hat{\alpha}_i \rightarrow g(x_i) \text{ and}$$

$$\hat{\beta}_i \rightarrow \frac{\partial g(x_i)}{\partial x_i}$$

for all i and for a sufficiently large n .

Proof. The uniqueness of the estimates of \hat{a}_i and \hat{b}_i is established because (6) is a quadratic programming problem with a positive definite (strictly convex) objective function with a feasible solution. See for Bertsekas, (1995).

Theorem 2.1 in Kuosmanen (2008) shows the Afriat inequalities with non-negativity of the slope parameters characterizes the set of all monotonic and concave functions. Thus, the SCKLS estimation (6) which imposes Afriat inequality for concavity constraints and non-negativity on \mathbf{b}_i has same solution as the unconstrained minimization problem, $\min_{a_i, \mathbf{b}_i} \sum_{i=1}^m \sum_{j=1}^n \left(y_j - a_i - (\mathbf{X}_j - \mathbf{x}_i)' \mathbf{b}_i \right)^2 K \left(\frac{\mathbf{X}_j - \mathbf{x}_i}{\mathbf{h}} \right)$. We can decompose the unconstrained minimization problem objective function into m local linear functional estimators at each evaluation point x_i .

$$\begin{aligned}
& \sum_{i=1}^m \sum_{j=1}^n \left(y_j - a_i - (\mathbf{X}_j - \mathbf{x}_i)' \mathbf{b}_i \right)^2 K \left(\frac{\mathbf{X}_j - \mathbf{x}_i}{\mathbf{h}} \right) \\
&= \sum_{j=1}^n \left(y_j - a_1 - (\mathbf{X}_j - \mathbf{x}_1)' \mathbf{b}_1 \right)^2 K \left(\frac{\mathbf{X}_j - \mathbf{x}_1}{\mathbf{h}} \right) \\
&+ \sum_{j=1}^n \left(y_j - a_2 - (\mathbf{X}_j - \mathbf{x}_2)' \mathbf{b}_2 \right)^2 K \left(\frac{\mathbf{X}_j - \mathbf{x}_2}{\mathbf{h}} \right) \\
&+ \dots \\
&+ \sum_{j=1}^n \left(y_j - a_m - (\mathbf{X}_j - \mathbf{x}_m)' \mathbf{b}_m \right)^2 K \left(\frac{\mathbf{X}_j - \mathbf{x}_m}{\mathbf{h}} \right)
\end{aligned} \tag{8}$$

Because the local linear estimator is consistent estimator under Assumption 1, and the true function g is a monotonic increasing concave function, that is, $g \in G_2$, then for sufficiently large n , the unconstrained minimization problem with objective function (8) results in a functional estimate

$\hat{g}_n(x; \hat{\mathbf{a}}, \hat{\mathbf{b}}) \in G_2$ with $\hat{a}_i \rightarrow g(x_i)$ and $\hat{b}_i \rightarrow \frac{\partial g(x_i)}{\partial x_i}$ for all i . ■

4.2. Special Cases of SCKLS

Theorem 1 establishes SCKLS is a consistent estimator. We will next consider a set of conditions under which the CNLS and SCKLS estimators are identical.

Assumption 2. *Assume that the set of evaluation points for the SCKLS estimator satisfies either of the following conditions:*

- (i). *The set of evaluation points are equal to sample input vectors, i.e. $\mathbf{x}_i = \mathbf{X}_i, i = 1, \dots, n$*
- (ii). *There are infinitely many points for evaluation and the density function for evaluation points is positive over a continuous and bounded region of the input space.*

Theorem 2. *Suppose that Assumption 2 holds. Then, when the bandwidth approaches zero, i.e. $h \rightarrow 0$, the objective function of the SCKLS estimator converges to the CNLS estimator.*

Proof. Under either condition of (i) or (ii) in Assumption 2, when $h \rightarrow 0$, we have

$$\frac{\mathbf{X}_j - \mathbf{x}_i}{\mathbf{h}} = \begin{cases} \infty & \text{if } \mathbf{x}_i \neq \mathbf{X}_j \\ 0 & \text{if } \mathbf{x}_i = \mathbf{X}_j \end{cases} \text{ for } i, j = 1, \dots, n$$

which implies

$$K\left(\frac{\mathbf{X}_j - \mathbf{x}_i}{\mathbf{h}}\right) \rightarrow \begin{cases} 0 & \text{if } \mathbf{x}_i \neq \mathbf{X}_j \\ c & \text{if } \mathbf{x}_i = \mathbf{X}_j \end{cases} \text{ for } i, j = 1, \dots, n$$

where c is a positive constant whose value depends on the type of kernel function. Then, the objective function of (6) converges to

$$\operatorname{argmin}_{a_j, \mathbf{b}_j} \sum_{j=1}^n (y_j - a_j)^2 c = \operatorname{argmin}_{a_j, \mathbf{b}_j} \sum_{j=1}^n (y_j - a_j)^2. \quad (9)$$

Here, $a_j = \alpha_j + \boldsymbol{\beta}'_j \mathbf{X}_j$ and $\mathbf{b}_j = \boldsymbol{\beta}_j$ for $j = 1, \dots, n$ by definition. Then, quadratic programming problem (6) can be rewritten as follows:

$$\begin{aligned} & \min_{a_j, \mathbf{b}_j} \sum_{j=1}^n (y_j - (\alpha_j + \boldsymbol{\beta}'_j \mathbf{X}_j))^2 \\ & \text{subject to} \\ & \alpha_j + \boldsymbol{\beta}'_j \mathbf{X}_j \leq \alpha_l + \boldsymbol{\beta}'_l \mathbf{X}_j \quad j, l = 1, \dots, n \\ & \boldsymbol{\beta}_j \geq 0 \quad j = 1, \dots, n \end{aligned} \quad (10)$$

which is equivalent to the formulation of the CNLS estimator (1). ■

Theorem 2 shows that if the bandwidth is small enough, then the SCKLS estimator is equivalent to the CNLS estimates. We can decompose Mean Squared Errors (MSE) into bias and variance as follows:

$$\begin{aligned} \text{MSE}(\hat{g}(x)) &= E[(g(x) - \hat{g}(x))^2] \\ &= (E[\hat{g}(x)] - g(x))^2 + E[(\hat{g}(x) - E[\hat{g}(x)])^2] \\ &= (\text{Bias})^2 + (\text{Variance}) \end{aligned} \quad (11)$$

where g is true function and \hat{g} is estimated function. Recognizing the bias/variance tradeoff commonly discussed in kernel methods, we note that the CNLS estimator's equivalence to the zero bandwidth SCKLS estimator implies that the CNLS estimator is the minimum bias estimator in the class of SCKLS estimators.

Theorem 3. *Suppose that Assumption 1 (i) holds. Then, CNLS is the minimum bias estimator in the class of SCKLS estimators.*

Proof. By Theorem 2, SCKLS is equivalent to CNLS as $\mathbf{h} \rightarrow 0$. As the vector of bandwidths, \mathbf{h} , approaches zero, the bias introduced by including observations distant from \mathbf{x}_i in the kernel calculation decreases. However, as Seijo and Sen (2011) show, while on average the shape constrained function is unbiased, the shape constraints may introduced bias for particular point estimates. Therefore, CNLS is the minimum bias estimator in the class of SCKLS estimators. ■

Theorems 2 and 3 shows that if the bandwidth is small enough and approaches zero, then the SCKLS estimator converges to the CNLS estimator which is on average unbiased. As in all kernel estimators when the bandwidth is reduced the bias decreases while the variance increases, and vice versa. Consequently, the SCKLS estimator can control this tradeoff through bandwidth selection.

Additional equivalence results can be shown. Theorem 4 shows the equivalence of linear regression subject to monotonicity constraints and the SCKLS estimator when bandwidth approaches to infinity.

Theorem 4. *When the bandwidth approaches to infinity, the SCKLS estimator converges to the least squares estimator of the linear regression model subject to monotonicity constraints.*

Proof. When $h \rightarrow \infty$, we have

$$\frac{\mathbf{X}_j - \mathbf{x}_i}{h} \rightarrow 0$$

which implies

$$K\left(\frac{\mathbf{X}_j - \mathbf{x}_i}{h}\right) \rightarrow c \quad (12)$$

where c is a positive constant whose value depends on the type of kernel function. By substituting (12) into the objective function of (6), it converges to

$$\begin{aligned} \operatorname{argmin}_{a_i, \mathbf{b}_i} \sum_{j=1}^n \left(y_j - a_i - (\mathbf{X}_j - \mathbf{x}_i)' \mathbf{b}_i \right)^2 c \\ = \operatorname{argmin}_{a_i, \mathbf{b}_i} \sum_{j=1}^n \left(y_j - a_i - (\mathbf{X}_j - \mathbf{x}_i)' \mathbf{b}_i \right)^2 \end{aligned} \quad (13)$$

Here, $a_j = \alpha_j + \boldsymbol{\beta}'_j \mathbf{X}_j$ and $\mathbf{b}_j = \boldsymbol{\beta}_j$ for $j = 1, \dots, n$ by the definition. Then quadratic programming problem (6) can be rewritten as follows with (13).

$$\begin{aligned} \min_{\alpha_i, \boldsymbol{\beta}_i} \sum_{i=1}^m \sum_{j=1}^n \left(y_j - (\alpha_i + \boldsymbol{\beta}'_i \mathbf{X}_j) \right)^2 \\ \text{subject to} \\ \alpha_i + \boldsymbol{\beta}'_i \mathbf{X}_i \leq \alpha_l + \boldsymbol{\beta}'_l \mathbf{X}_i \quad i, l = 1, \dots, m \\ \boldsymbol{\beta}_i \geq 0 \quad i = 1, \dots, m \end{aligned} \quad (14)$$

Here, since we do not impose any weight on the objective function, α_i and $\boldsymbol{\beta}_i$ must be constant for $i = 1, \dots, m$. Then the first constraint of (14) becomes redundant, resulting in

$$\begin{aligned} \min_{\alpha, \boldsymbol{\beta}} \sum_{j=1}^n \left(y_j - (\alpha + \boldsymbol{\beta}' \mathbf{X}_j) \right)^2 \\ \text{subject to} \\ \boldsymbol{\beta} \geq 0 \end{aligned} \quad (15)$$

Which is equivalent to linear regression subject to monotonicity. ■

5. Monte Carlo Simulations

In this section, we examine finite sample performance and robustness of the proposed estimator through a series of Monte Carlo simulations. We run those experiments on a personal computer with Intel Core2 Quad CPU 3.00 GHz and 8GB RAM. For the SCKLS and CNLS estimator, we solve the quadratic programming problems with MATLAB using the built-in quadratic programming solver, *quadprog*. For the CWB estimator, we use the convex optimization solver called *SeDuMi* because *quadprog* was not able to solve CWB.⁵ We run 4 sets of experiments varying the size of noise, the distribution of the input variables, and investigating the effects of a non-uniform grid for imposing the convexity/concavity constraints. Experiment 1 considers uniformly distributed input variables to compare the basic performance of the SCKLS, CWB and CNLS estimator. Experiment 2 increases the noise level in the data generation process. Experiment 3 considers non-uniform distributed input variables to validate the robustness and the benefits of the extension of SCKLS: variable bandwidth with k-NN approach and non-uniform grid. Finally, we run Experiment 4 with uniform input and vary the number of evaluation points to assess how the number of evaluation points affect the performance and computational difficulty of SCKLS and CWB estimator.

For both SCKLS and CWB estimators, we use Gaussian kernel function $K(\cdot)$ and leave-one-out cross-validation (LOOCV) method for bandwidth selection. LOOCV is completely data-driven method, and has been shown to perform well for unconstrained kernel estimator such as local linear (Stone (1977)). To improve the computational performance, we apply the iterative algorithm described in Appendix C to both SCKLS and CWB estimators. For CWB estimator, we use a local linear estimator to obtain the weighting matrix $A_i(\mathbf{x})$ in (2). The first partial derivative

⁵ For the CWB estimator, the *SeDuMi* solver provides a better solution than the *quadprog* solver while both the *SeDuMi* and the *quadprog* solver have same solution for SCKLS estimator.

of $\hat{g}(\mathbf{x}|p)$ is obtained by approximating the derivatives through numerical differentiation

$$\hat{g}^{(1)}(\mathbf{x}|p) = \frac{\hat{g}(\mathbf{x} + \Delta|p) - \hat{g}(\mathbf{x}|p)}{\Delta} \text{ where } \Delta \text{ is a small positive constant.}^6$$

We measure the estimator's performance using Root Mean Squared Errors (RMSE) based on two criteria: the distance from the estimated function to the true function measured 1) at the observed points and 2) at the evaluation points respectively. CNLS estimates piece-wise hyperplanes on observation points and SCKLS estimates on evaluation points. We use linear interpolation to obtain the RMSE of CNLS⁷ and SCKLS on evaluation points and observation points respectively. We also measure how the iterative algorithm for SCKLS helps alleviate computational difficulty by reporting the percentage of constraints which are used to obtain the optimal solution and the computational time in seconds. We do not use the constraint reduction algorithm for CNLS. We replicate each scenario 10 times and report the average.

5.1. Experiment 1: Uniform input

Experiment 1: We consider a Cobb-Douglas production function with d -inputs and one-output,

$$y = \prod_{k=1}^d x_k^{\frac{0.8}{d}} + \epsilon, \text{ where each observed input } x_k \text{ is randomly drawn from uniform distribution,}$$

$unif[1,10]$, and noise, ϵ , is randomly sampled from a normal distribution, $N(0,0.7^2)$. We

consider 15 different scenarios with different numbers of observations (100, 200, 300, 400 and 500) and input dimension (2, 3 and 4). The structure and data generation process of Experiment 1 follows Lee et al. (2013). The number of evaluation points is fixed at 400, and set as uniform grid.

⁶ Du et al. (2013) proposes to use an analytical derivative for the first partial derivative of $\hat{g}(\mathbf{x}|p)$; however, our experiments indicate the use of an analytical derivative leads to unstable performance as summarized in Appendix A.

⁷ The CNLS estimates include the second stage linear programming estimation procedure described in Kuosmanen and Kortelainen (2012) to find the minimum extrapolated production function.

For this experiment, we compare the following five estimators: SCKLS with fixed bandwidth, CNLS, CWB in p-space, Local Linear Kernel, and parametric Cobb-Douglas function. Table 1 and Table 2 show for Experiment 1 the RMSE measured on observation points and evaluation points respectively. The number in parentheses is the standard deviation calculated from 10 replications. Note the standard deviation are generally small compared to the parameter estimates indicating even after only 10 replications the variability in the estimates is low. A more extensive set of results for this experiment is summarized in Appendix D. The SCKLS estimator has the lowest root RMSE in most scenarios even when RMSE is measured on observation points (note the SCKLS estimator imposes the shape constraints on evaluation points). Also as expected, the performance of SCKLS estimator improves as the number of observation points increases. Moreover, the SCKLS estimator performs better than the Local Linear estimator particularly in higher dimensional functional estimation. Thus, providing empirically evidence that the shape constraints in the SCKLS estimator are helpful to improve the finite sample performance. The Local Linear estimator has larger RMSE values on evaluation points which are located in input space regions with sparse observations. Therefore, the SCKLS estimator has more robust out-of-sample performance than the Local Linear estimator due to the shape constraints. We also observe that the performance of the CNLS estimator deteriorates when RMSE is measured at the evaluation points. CNLS often has ill-defined hyperplanes which are very steep/shallow at the edge of the observed data, this over fitting leads to poor out-of-sample performance. In contrast, the SCKLS estimator performs similarly for both the observation points and evaluation points due to the construction of the grid that completely covers the observed data making the SCKLS estimator more robust. Although the SCKLS and the CWB estimators are relatively competitive when the

number of observations is large, the SCKLS estimator has significantly better performance when the observations are small.

Table 3 shows the computational time of Experiment 1 for the shape constrained estimators which are more computationally intensive than the Local Linear estimator. The value inside parenthesis indicates the percentage of constraints included in the optimization problem that resulted in the optimal solution. While CNLS is the fastest estimator when the number of observations is small, the SCKLS estimator is faster in the case of larger datasets or high dimensional scenarios. Since we alleviate the curse of dimensionality by using the iterative algorithm, we can analyze larger dataset to estimate production function. The iterative algorithm is more effective for estimating low dimensionality functions because in higher dimensional spaces the number of adjacent grid points is relatively large.

Table 1. RMSE on observation points for Experiment 1

Number of observations	Average of RMSE on observation points					
	100	200	300	400	500	
2-input	SCKLS fixed bandwidth	0.193 (0.053)	0.171 (0.047)	0.141 (0.032)	0.132 (0.029)	0.118 (0.017)
	CNLS	0.229 (0.042)	0.163 (0.037)	0.137 (0.010)	0.138 (0.027)	0.116 (0.016)
	CWB in p-space	0.189 (0.055)	0.167 (0.049)	0.158 (0.040)	0.140 (0.026)	0.129 (0.019)
	Local Linear	0.212 (0.079)	0.166 (0.042)	0.149 (0.028)	0.152 (0.028)	0.140 (0.028)
	Cobb-Douglas	0.078	0.075	0.048	0.039	0.043
3-input	SCKLS fixed bandwidth	0.230 (0.050)	0.187 (0.026)	0.183 (0.032)	0.152 (0.019)	0.165 (0.031)
	CNLS	0.294 (0.048)	0.202 (0.035)	0.189 (0.020)	0.173 (0.014)	0.168 (0.020)
	CWB in p-space	0.228 (0.043)	0.221 (0.039)	0.210 (0.037)	0.183 (0.040)	0.172 (0.024)
	Local Linear	0.250 (0.068)	0.230 (0.050)	0.235 (0.052)	0.203 (0.050)	0.181 (0.021)
	Cobb-Douglas	0.104	0.089	0.070	0.047	0.041
4-input	SCKLS fixed bandwidth	0.225 (0.038)	0.248 (0.020)	0.228 (0.037)	0.203 (0.042)	0.198 (0.028)
	CNLS	0.315 (0.039)	0.294 (0.027)	0.246 (0.024)	0.235 (0.029)	0.214 (0.015)
	CWB in p-space	0.238 (0.038)	0.262 (0.056)	0.231 (0.039)	0.234 (0.076)	0.198 (0.030)
	Local Linear	0.256 (0.044)	0.297 (0.057)	0.252 (0.056)	0.240 (0.060)	0.226 (0.038)
	Cobb-Douglas	0.120	0.073	0.091	0.067	0.063

Table 2. RMSE on evaluation points for Experiment 1

Number of observations	Average of RMSE on evaluation points					
	100	200	300	400	500	
2-input	SCKLS fixed bandwidth	0.219 (0.053)	0.189 (0.057)	0.150 (0.034)	0.147 (0.030)	0.128 (0.021)
	CNLS	0.350 (0.082)	0.299 (0.093)	0.260 (0.109)	0.284 (0.119)	0.265 (0.078)
	CWB in p-space	0.206 (0.049)	0.186 (0.062)	0.174 (0.043)	0.154 (0.026)	0.143 (0.021)
	Local Linear	0.247 (0.101)	0.182 (0.053)	0.167 (0.030)	0.171 (0.030)	0.156 (0.034)
	Cobb-Douglas	0.076	0.076	0.049	0.040	0.043
3-input	SCKLS fixed bandwidth	0.283 (0.072)	0.231 (0.033)	0.238 (0.030)	0.213 (0.029)	0.215 (0.034)
	CNLS	0.529 (0.112)	0.587 (0.243)	0.540 (0.161)	0.589 (0.109)	0.598 (0.143)
	CWB in p-space	0.291 (0.069)	0.289 (0.052)	0.269 (0.035)	0.252 (0.052)	0.233 (0.031)
	Local Linear	0.336 (0.085)	0.340 (0.093)	0.360 (0.108)	0.326 (0.086)	0.264 (0.042)
	Cobb-Douglas	0.116	0.098	0.080	0.052	0.046
4-input	SCKLS fixed bandwidth	0.321 (0.046)	0.357 (0.065)	0.329 (0.049)	0.308 (0.084)	0.290 (0.044)
	CNLS	0.845 (0.188)	0.873 (0.137)	0.901 (0.151)	0.827 (0.235)	0.792 (0.091)
	CWB in p-space	0.360 (0.039)	0.385 (0.077)	0.358 (0.068)	0.361 (0.138)	0.325 (0.077)
	Local Linear	0.482 (0.115)	0.527 (0.125)	0.483 (0.146)	0.495 (0.153)	0.445 (0.074)
	Cobb-Douglas	0.146	0.091	0.115	0.081	0.080

Table 3. Computational time for Experiment 1

Number of observations		The average computational time in seconds; (percentage of Afriat constraints included in the final optimization problem)				
		100	200	300	400	500
2-input	SCKLS fixed bandwidth	14.1 (6.14%)	13.3 (5.28%)	42.2 (8.86%)	34.7 (7.80%)	77.4 (8.31%)
	CNLS	2.0 (100%)	6.1 (100%)	16.5 (100%)	26.5 (100%)	55.3 (100%)
	CWB in p-space	24.1 (2.39%)	33.2 (2.35%)	76.6 (2.35%)	82.3 (2.35%)	130 (2.35%)
3-input	SCKLS fixed bandwidth	26.9 (16.0%)	40.4 (16.6%)	45.5 (16.3%)	67.3 (16.4%)	136 (16.2%)
	CNLS	3.8 (100%)	16.4 (100%)	37.0 (100%)	82.9 (100%)	161 (100%)
	CWB in p-space	47.6 (15.5%)	71.5 (15.5%)	100 (15.5%)	202 (15.5%)	255 (15.5%)
4-input	SCKLS fixed bandwidth	47.5 (40.1%)	71.6 (39.9%)	77.4 (39.9%)	166 (40.0%)	235 (39.8%)
	CNLS	5.8 (100%)	22.4 (100%)	79.1 (100%)	139.8 (100%)	287.8 (100%)
	CWB in p-space	68.8 (39.8%)	136 (39.8%)	196 (39.8%)	327 (39.8%)	442 (39.8%)

5.2. Experiment 2: Uniform input with noisy data

Experiment 2: We consider a Cobb-Douglas production function with d -inputs and one-output,

$y = \prod_{k=1}^d x_k^{\frac{0.8}{d}} + \epsilon$, where each observed input x_k is randomly drawn from uniform distribution,

$unif[1,10]$, and noise, ϵ , is randomly sampled from a normal distribution, $N(0,1.3^2)$. We

consider 15 different scenarios with different numbers of observations (100, 200, 300, 400 and

500) and input dimension (2, 3 and 4). The number of evaluation points is fixed at 400, and set as

uniform grid. This experiment has a higher noise level in the data generation process relative to

Experiment 1.

For this experiment, we compare the same five estimators: SCKLS with fixed bandwidth, CNLS, CWB in p-space, Local Linear Kernel, and parametric Cobb-Douglas function. Table 4

and Table 5 summarizes the estimators' performance for Experiment 2 in terms of RMSE measured on observation points and evaluation points respectively. The comprehensive results of this experiment is summarized at Appendix E. In contrast to Experiment 1, CWB is not stable and not very competitive relative to the SCKLS estimator. This indicates that the SCKLS estimator is more robust to the noise in data than CWB estimator. The CWB estimator first estimates the unconstrained kernel weighted estimator, and this first stage estimate can deviate from the true function significantly in the high noise scenarios. Because the second stage of the CWB estimator identifies the shape restricted function as close as possible to the unrestricted estimator, a poor estimate in the first stage leads to poor performance of the CWB estimator overall. In contrast, the SCKLS estimator estimates directly the constrained function, and thus, can mitigate the effects from noise in data.

Table 4. RMSE on observation points for Experiment 2

Number of observations		Average of RMSE on observation points				
		100	200	300	400	500
2-input	SCKLS fixed bandwidth	0.239	0.203	0.203	0.155	0.140
	CNLS	0.279	0.231	0.194	0.168	0.151
	CWB in p-space	0.314	0.215	0.237	0.275	0.151
	Local Linear	0.287	0.244	0.230	0.214	0.161
	Cobb-Douglas	0.109	0.108	0.081	0.042	0.048
3-input	SCKLS fixed bandwidth	0.292	0.263	0.221	0.204	0.184
	CNLS	0.379	0.303	0.275	0.224	0.214
	CWB in p-space	0.318	0.306	0.308	0.244	0.214
	Local Linear	0.333	0.306	0.288	0.259	0.214
	Cobb-Douglas	0.176	0.118	0.101	0.084	0.072
4-input	SCKLS fixed bandwidth	0.317	0.291	0.249	0.241	0.254
	CNLS	0.491	0.356	0.311	0.293	0.313
	CWB in p-space	0.400	0.318	0.273	0.260	0.289
	Local Linear	0.335	0.342	0.257	0.274	0.283
	Cobb-Douglas	0.157	0.150	0.112	0.075	0.077

Table 5. RMSE on evaluation points for Experiment 2

Number of observations		Average of RMSE on evaluation points				
		100	200	300	400	500
2-input	SCKLS fixed bandwidth	0.253	0.225	0.222	0.172	0.160
	CNLS	0.319	0.355	0.334	0.255	0.267
	CWB in p-space	0.329	0.239	0.262	0.305	0.177
	Local Linear	0.330	0.272	0.257	0.239	0.194
	Cobb-Douglas	0.112	0.112	0.083	0.044	0.049
3-input	SCKLS fixed bandwidth	0.367	0.339	0.302	0.268	0.231
	CNLS	0.743	0.778	0.744	0.696	0.620
	CWB in p-space	0.398	0.392	0.434	0.336	0.274
	Local Linear	0.452	0.444	0.438	0.398	0.302
	Cobb-Douglas	0.202	0.130	0.110	0.093	0.079
4-input	SCKLS fixed bandwidth	0.405	0.460	0.349	0.350	0.347
	CNLS	1.019	0.950	0.985	1.043	1.106
	CWB in p-space	0.514	0.520	0.393	0.390	0.452
	Local Linear	0.524	0.626	0.451	0.491	0.550
	Cobb-Douglas	0.187	0.194	0.134	0.092	0.091

5.3. Experiment 3: Non-uniform input

Experiment 3: We consider a Cobb-Douglas production function with d -inputs and one-output,

$$y = \prod_{k=1}^d x_k^{\frac{0.8}{d}} + \epsilon, \text{ where } \epsilon \text{ and random noise } \epsilon \text{ is randomly sampled from a normal distribution,}$$

$N(0, 0.7^2)$. The input, x_k , is randomly drawn from truncated exponential distribution, $\exp(3) \cdot$

$I(x_k \in [1, 10])$ where $I(\cdot)$ denotes the indicator function which take the value 1 when the

statement in the parenthesis is true and 0 otherwise. Each input for each observation is generated

in the same way. We consider 15 different scenarios with different numbers of observations (100,

200, 300, 400 and 500) and input dimension (2, 3 and 4). The number of evaluation point is fixed

at 400, and set as non-uniform grid. Note this experiment only differs from Experiment 1 in that

the distribution of inputs is skewed and thus non-uniform.

For this experiment, we compare the performance of SCKLS estimator with different

extensions: SCKLS with fixed bandwidth, with variable bandwidth (k-NN) and with non-uniform

grid. Table 6 and Table 7 show the RMSE of Experiment 3 on observation points and evaluation

points respectively. The comprehensive results of this experiment is summarized at Appendix F. A uniform grid is used like in Experiment 1. As the dimension of input space and the number of observations increase, SCKLS with variable bandwidth performs better than the fixed bandwidth estimator. SCKLS with non-uniform grid performs better than SCKLS with uniform grid for almost all scenarios since DGP has non-uniform input. Consequently, we conclude that variable bandwidth methods, such as k-NN approach, and non-uniform grid are useful to handle non-uniform input data which is common feature of real data especially when the large data set is available.

Table 6. RMSE on observation points for Experiment 3

Number of observations		Average of RMSE on observation points				
		100	200	300	400	500
2-input	SCKLS fixed/uniform	0.179	0.151	0.144	0.121	0.108
	SCKLS variable/uniform	0.183	0.156	0.142	0.125	0.104
	SCKLS variable/non-uniform	0.176	0.144	0.132	0.114	0.093
3-input	SCKLS fixed/uniform	0.197	0.184	0.172	0.164	0.167
	SCKLS variable/uniform	0.212	0.187	0.170	0.175	0.170
	SCKLS variable/non-uniform	0.210	0.180	0.162	0.160	0.155
4-input	SCKLS fixed/uniform	0.219	0.211	0.196	0.209	0.187
	SCKLS variable/uniform	0.208	0.193	0.167	0.171	0.170
	SCKLS variable/non-uniform	0.206	0.193	0.164	0.169	0.168

Table 7. RMSE on evaluation points for Experiment 3

Number of observations		Average of RMSE on evaluation points				
		100	200	300	400	500
2-input	SCKLS fixed/uniform	0.262	0.220	0.244	0.157	0.196
	SCKLS variable/uniform	0.246	0.204	0.192	0.142	0.136
	SCKLS variable/non-uniform	0.193	0.160	0.145	0.120	0.100
3-input	SCKLS fixed/uniform	0.323	0.308	0.311	0.286	0.293
	SCKLS variable/uniform	0.335	0.303	0.281	0.262	0.254
	SCKLS variable/non-uniform	0.278	0.243	0.219	0.212	0.196
4-input	SCKLS fixed/uniform	0.406	0.398	0.397	0.404	0.400
	SCKLS variable/uniform	0.417	0.423	0.368	0.364	0.356
	SCKLS variable/non-uniform	0.359	0.359	0.313	0.302	0.280

5.4. Experiment 4: Uniform input with different evaluation points

Experiment 4: The DGP is exactly same as Experiment 1. However, now we consider 9 different scenarios with different numbers of evaluation points (100, 300, and 500) and input dimension (2, 3 and 4). The number of observations is fixed at 400. The evaluation points are constructed on a uniform grid.

We compare following two estimators: SCKLS with fixed bandwidth, CWB in p-space. Table 8 and Table 9 shows for Experiment 4 the RMSE measured on observations and evaluation points respectively. The comprehensive results of this experiment is summarized at Appendix G. The SCKLS estimator outperforms the CWB estimator for almost all scenarios. Table 8 shows that even if we increase the number of evaluation points, the RMSE value does not change significantly. Thus, we conclude that the SCKLS estimator performs well even on a relatively rough grid of points. This has implications for the computational run time, specifically, we can reduce the calculation time by using a rough grid without sacrificing much in terms of performance of the estimator.

Table 10 summarizes the computational times for Experiment 4 and shows the percentage of constraints used for each estimator. The SCKLS estimator can always be calculated faster than the CWB estimator. When the dimensionality of the input space is low, the number of evaluation points does not affect the computational time much because the iterative algorithm reduce the number of constraints significantly. However, when the dimensionality is high, the large number of adjacent grid points creates a large number of constraints and thus a single quadratic program takes a long time to solve. Summarizing the results from Experiment 4, we recommend using a rough grid in high dimensional input data cases to keep computational times reasonably short.

Table 8. RMSE on observation points for Experiment 4

Number of evaluation points		Average of RMSE on observation points		
		100	300	500
2-input	SCKLS fixed bandwidth	0.142	0.141	0.141
	CWB in p-space	0.149	0.151	0.156
3-input	SCKLS fixed bandwidth	0.198	0.203	0.197
	CWB in p-space	0.218	0.234	0.231
4-input	SCKLS fixed bandwidth	0.239	0.207	0.206
	CWB in p-space	0.219	0.227	0.296

Table 9. RMSE on evaluation points for Experiment 4

Number of evaluation points		Average of RMSE on evaluation points		
		100	200	300
2-input	SCKLS fixed bandwidth	0.181	0.164	0.158
	CWB in p-space	0.195	0.180	0.179
3-input	SCKLS fixed bandwidth	0.304	0.267	0.257
	CWB in p-space	0.332	0.329	0.302
4-input	SCKLS fixed bandwidth	0.383	0.296	0.270
	CWB in p-space	0.403	0.359	0.415

Table 10. Computational time for Experiment 4

Number of evaluation points		Average of computational time in seconds; (percentage of Afriat constraints included in the final optimization problem)		
		100	300	500
2-input	SCKLS fixed bandwidth	26.6 (11.7%)	28.3 (6.56%)	34.0 (5.45%)
	CWB in p-space	41.0 (8.77%)	56.5 (3.21%)	74.2 (1.95%)
3-input	SCKLS fixed bandwidth	84.8 (29.1%)	112 (16.7%)	134 (13.3%)
	CWB in p-space	121 (28.2%)	221 (15.5%)	310 (12.2%)
4-input	SCKLS fixed bandwidth	149 (62.3%)	170 (40.0%)	597 (27.7%)
	CWB in p-space	175 (61.9%)	275 (39.8%)	729 (27.4%)

6. Application

We apply the proposed method to estimate the production function for two large industries in Chile: plastic (2520) and wood manufacturing (2010) where the values inside the parentheses indicate CIIU3 industry code. There are some existing studies which analyze the productivity of

Chilean data, see for example Pavcnik (2002). She analyzed how trade liberalization affects the productivity improvements. Other researchers have analyzed the productivity of Chilean manufacturing such as Benavente (2006), Benavente and Ferrade (2003) and De Loecker, J. (2007). However, these previous researches use strong parametric assumptions and older data. Here, we relax the parametric assumptions and estimate a shape constrained production function nonparametrically for 2010 data. We examine the marginal productivity, marginal rate of substitution, time fixed effect and most productive scale size (MPSS) to analyze the structure and growth using nonparametric estimation. Furthermore, exporting has become more important source of revenue in Chile for recent years. Here we investigate that how productivity differs between exporting and non-exporting firms.

6.1. The census of Chilean manufacturing plants

This paper uses the Chilean Annual Industrial Survey which is provided by National Institute of Statistics in Chile. The survey of the census covers manufacturing establishments with ten or more employees. We define Capital, X_k , and Labor, X_l , as the input variables and Value Added, y , as the output variable of the production function. Capital and Value Added are measured in millions of Chilean peso and Labor is measured as the total of man-hours per year. We use cross sectional data from two large industries in Chilean manufacturing industry: plastic and wood.

Many researchers have found positive effects of exporting for other countries using parametric models, De Loecker (2007) and Bernard and Jensen (2004), we relax the parametric assumption for the production function by using the SCKLS estimator. To capture the effects of exporting, we use a semi-parametric modeling extension of SCKLS described in Appendix H, see also Robinson (1988). We model exporting with two variables: a dummy variable indicating the

establishments that are exporting and the share of output being exported. Our empirical results indicate exporting establishments are more productive than non-exporters establishments.

Table 11 presents the summary of statistics for each industry by exporter/non-exporter. We find that exporters are typically larger than non-exporter in terms of labor and capital. Input variables are positively skewed, indicating there exist many small and few large establishments. Because SCKLS with variable bandwidth (k-NN) and non-uniform grid performed the best in the simulation scenarios with non-uniform input data, we use that method for analysis.

Figure 3 is a plot of labor and capital for each industry. We find that input data is very spares for large establishments. Beresteanu (2005) proposed to include shape constraints only for the evaluation points that contain at least one observation within a gridded square. So in addition to using a non-uniform grid of evaluation points, we also apply Beresteanu criteria to avoid using redundant evaluation points and over smoothing.

Table 11. Statistics of Chilean manufacturing data

Plastic (2520)	Non-exporters ($n = 173$)			Exporters ($n = 72$)			
	Labor	Capital (million)	Value Added (million)	Labor	Capital (million)	Value Added (million)	Share of Exports
Mean	92155	725.85	546.93	240890	2859	1733.9	0.147
Median	55220	258.41	247.05	180330	1329.1	1054.9	0.0524
St. dev	106530	1574	1068.1	212480	3840.2	1678.8	0.201
Skewness	3.301	5.2052	5.9214	1.3681	2.4594	1.0678	-0.303
Wood (2010)	Non-exporters ($n = 97$)			Exporters ($n = 35$)			
	Labor	Capital	Value Added	Labor	Capital	Value Added	Share of Exports
Mean	76561	364.93	334.83	501470	3063.4	4524.1	0.542
Median	44087	109.48	115.39	378000	2195.4	2673.5	0.648
St. dev	78057	702.35	555.87	436100	2510.3	4466.3	0.355
Skewness	2.243	3.5155	3.432	0.81454	0.63943	1.0556	-0.303

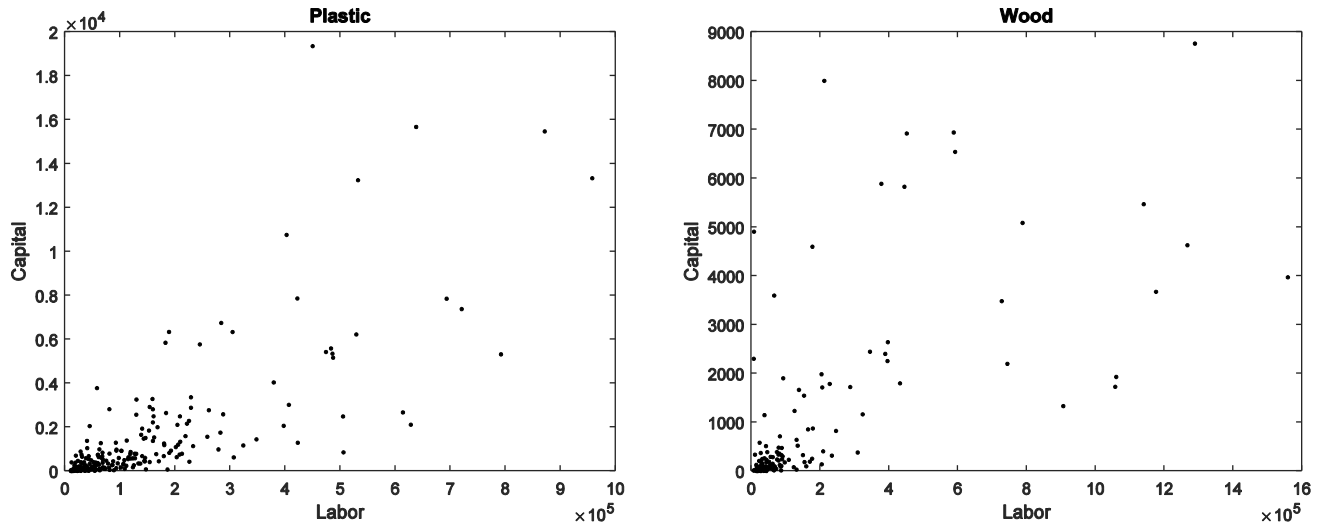


Figure 3. Labor and Capital of each industry

6.2. Estimated production function and interpretation

We estimate a semi-parametric model with a nonparametric shape constrained production function and a linear model for exporting share of sales and a dummy variables of exporting. Table 12 shows the goodness of fit of production function: 71.1% of variance is explained in plastic industry while 43.8% of variance is explained in wood industry.

Table 13 reports additional information characterizing the production function: the marginal productivity and the marginal rate of substitution at the 0, 10, 25, 50, 75, 90, 100 percentile is reported for both measures. Here, the rate of substitution indicates that how much labor is required to maintain the same level of output when we decrease a unit of capital. Figure 4 is a graph of the estimated production function. Comparing the two industries, the wood industry has a larger marginal rate of substitution than the plastic industry. This indicates that capital is more critical in wood industry than plastic industry. This result is also apparent in Figure 4, the production function of wood industry is not sensitive to changes in labor.

Table 12. SCKLS fitting statistics for Cross Sectional data

Industry	Number of observations	Fraction of variance explained	Fraction of variance not explained
Plastic	245	71.1%	28.9%
Wood	132	43.8%	56.2%

Table 13. Characteristics of production function

Plastic (2520)			
	Marginal Productivity		Marginal Rate of Substitution (= b_k/b_l)
	Labor (= b_l) (million peso/employee)	Capital (= b_k) (peso/peso)	
0 th percentile	0.000182	3.45×10^{-15}	1.89×10^{-11}
10 th percentile	0.00396	0.111	23.3
25 th percentile	0.00523	0.139	23.9
50 th percentile	0.00579	0.139	24.0
75 th percentile	0.00579	0.139	35.3
90 th percentile	0.00579	0.260	44.8
100 th percentile	0.160	7.46	1288

Wood (2010)			
	Marginal Productivity		Marginal Rate of Substitution (= b_k/b_l)
	Labor (= b_l) (million peso/employee)	Capital (= b_k) (peso/peso)	
0 th percentile	3.89×10^{-20}	0.194	82.9
10 th percentile	1.46×10^{-18}	0.816	760
25 th percentile	8.55×10^{-16}	0.816	760
50 th percentile	0.00133	1.01	760
75 th percentile	0.00133	1.01	9.73×10^{14}
90 th percentile	0.00133	1.01	5.59×10^{17}
100 th percentile	0.0370	11.8	2.10×10^{19}

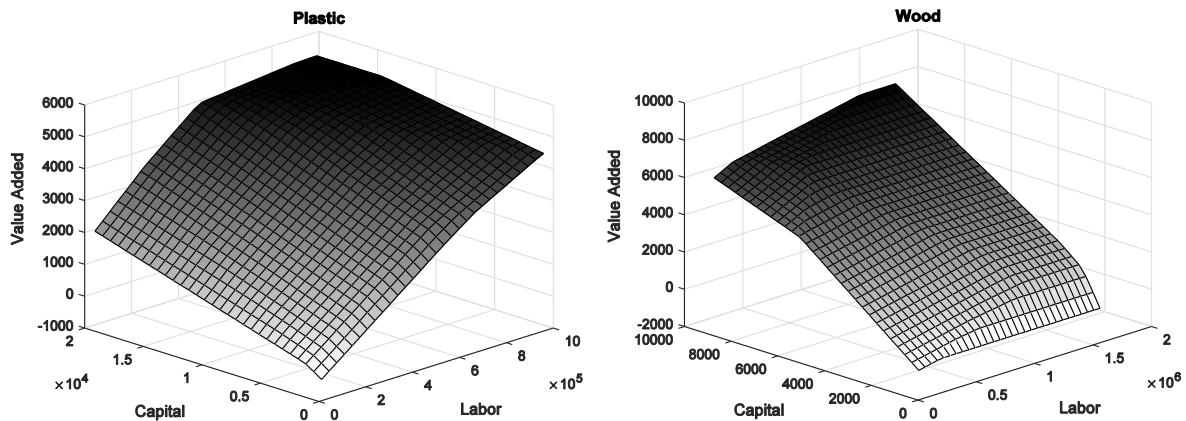


Figure 4. Estimated Production Function

Table 14 reports the coefficients estimate for the exporting variables. In the plastic industry, the dummy variable for exporting is significant and positive while exports' share of sales is not. This indicates that the plants that export tend to produce more output than plants who do not export regardless of the export quantity. In contrast, the coefficient on the exports' share of sales is significant and positive in wood industry while dummy variable for exporting is not significant indicating the establishments in wood industry tend to be more productive the more they export. Thus in both industries we find evidence of increased productivity for exporting firms.

Table 14. Coefficient of contextual variables

	Plastic (2520)		Wood (2010)	
	Dummy of exporting	Share of exporting in sales	Dummy of exporting	Share of exporting in sales
Point estimate	334.5	303.7	-763.0	4,114
95% lower bound	148.7	-334.3	-1944	2,568
95% upper bound	520.3	941.8	417.7	5,660
p-value	4.70×10^{-4}	0.349	0.203	5.64×10^{-7}

Table 15 reports the most productive scale size for the 10, 25, 50 75, 90 percentiles of Capital/Labor ratio distribution of observed input. In both industries, the observed value added output is the largest for establishments with high capital to labor ratios indicating capital intensive establishments have increased actual output. Furthermore, labor intensive establishments have smaller most productive scale size in both industries. This is consistent with the theory of the firm in which firms grow and become more labor intensive over time by automating processes with capital and using less labor.

Table 15. Most Productive Scale Size for each Capital/Labor ratio

Plastic (2520)			
Capital/Labor percentile	MPSS Labor	MPSS Capital	Output (Value added)
10 th percentile	619,580	519.1	3,290
25 th percentile	529,980	1,344	3,010
50 th percentile	529,980	2,604	3,185
75 th percentile	529,980	5,617	3,602
90 th percentile	529,980	10,270	4,248
Wood (2010)			
Capital/Labor percentile	MPSS Labor	MPSS Capital	Output (Value added)
10 th percentile	2,531,100	741.6	1,659
25 th percentile	1,045,000	1,200	2,142
50 th percentile	867,250	2,712	3,470
75 th percentile	662,700	4,179	4,682
90 th percentile	458,150	5,644	5,893

7. Conclusion

This paper proposed the SCKLS estimator that imposes shape constraints on a kernel estimator. We show the relationship between this new estimator and both CNLS and CWB. Specifically, we prove that CNLS is a minimum bias estimator in the class of SCKLS estimator. Thus, in applications where out-of-sample performance is less critical, such as regulation applications, the CNLS estimator might be preferred due to this minimum biased characteristic. In contrast, the case where out-of-sample performance is important, such as survey data, the SCKLS estimator is more robust. Simulation results reveal the SCKLS estimator outperforms existing estimators CNLS and CWB in most scenarios. In addition, we validate the usefulness of several extensions, including variable bandwidth and non-uniform gridding, are important to estimate function with non-uniform input data set which is common in manufacturing survey and census data. Finally, we demonstrate the SCKLS estimator empirically using Chilean manufacturing data. We compute marginal productivity, marginal rate of substitution, most productive scale size and

the effects of exporting, and provide several economic insights to the Chilean plastic and wood manufacturing.

One of the limitations of SCKLS estimator is its computation difficulty because of the large number of constraints. The algorithm we proposed for reducing constraints performs well, and we demonstrate the ability to solve large problems instances within a reasonable time periods. Furthermore, simulation results show good functional estimates even with a rough grid. Consequently, we can make use of the flexibility of the evaluation points to control the computational time of the estimator.

Potential future research should focus on the bandwidth selection methods. Typically, optimal bandwidth selection methods try to trade bias and variance to find the best estimator in terms of RMSE. Since the shape constraints already constrain the variance of the estimator to some extent, we expect that the optimal bandwidth in the SCKLS estimator will be smaller than the optimal unconstrained estimator. Further, if systematic inefficiency is present in the data, deconvoluting the residuals following the stochastic frontier literature would allow the investigation of a production frontier.

References

- Afriat, S.N. (1972). Efficiency estimation of production functions. *International Economic Review* 13(3): 568–598.
- Banker, R. D., & Maindiratta, A. (1992). Maximum likelihood estimation of monotone and concave production frontiers. *Journal of Productivity Analysis*, 3(4), 401-415.
- Benavente, J. M. (2006). The role of research and innovation in promoting productivity in Chile. *Economics of Innovation and New Technology*, 15(4-5), 301-315.

- Benavente, J. M., & Ferrada, C. (2003). Probability of survival of new manufacturing plants: the case of Chile. *Working paper*, Universidad de Chile.
- Beresteanu, A. (2005). Nonparametric analysis of cost complementarities in the telecommunications industry. *RAND Journal of Economics*, 870-889.
- Bernard, A. B., & Jensen, J. B. (2004). Exporting and Productivity in the USA. *Oxford Review of Economic Policy*, 20(3), 343-357.
- Bertsekas, D.P. (1995). *Nonlinear Programming*, Athena Scientific, 2nd Edition.
- Birke, M., Dette, H. (2007). Estimating a convex function in nonparametric regression. *Scandinavian Journal of Statistics*. 34: 384–404.
- Brunk, H.D. (1955). Maximum likelihood estimates of monotone parameters. *Annals of Mathematical Statistics* 26: 607–616.
- Carroll, R.J., Delaigle, A., Hall, P. (2011). Testing and estimating shape-constrained nonparametric density and regression in the presence of measurement error. *Journal of the American Statistical Association*, 106(493): 191–202.
- Cleveland, W. S. (1979). Robust locally weighted regression and smoothing scatterplots. *Journal of the American Statistical Association*, 74(368), 829-836.
- De Loecker, J. (2007). Do exports generate higher productivity? Evidence from Slovenia. *Journal of international economics*, 73(1), 69-98.
- Du, P., Parmeter, C.F., Racine, J.S. (2013). Nonparametric kernel regression with multiple predictors and multiple shape constraints. *Statistica Sinica* 23(3): 1347–1371.
- Grenander, U. (1956). On the theory of mortality measurement. *Scandinavian Actuarial Journal* 39(2): 70–96.

- Groeneboom, P., G. Jongbloed, and J.A. Wellner (2001). Estimation of a convex function: characterizations and asymptotic theory. *Annals of Statistics* 29:1653–1698.
- Hall, P., Huang, L.-S. (2001). Nonparametric kernel regression subject to monotonicity constraints. *Annals of Statistics* 29(3): 624–647.
- Hanson, D.L. and G. Pledger (1976). Consistency in concave regression. *Annals of Statistics* 4(6): 1038–1050.
- Hildreth, C. (1954). Point estimates of ordinates of concave functions. *Journal of the American Statistical Association* 49: 598–619.
- Holloway, C.A. (1979). On the estimation of convex functions. *Operations Research* 27(2):401–407.
- Kuosmanen, T. (2008). Representation theorem for convex nonparametric least squares. *Econometrics Journal* 11: 308–325.
- Kuosmanen, T., and M. Kortelainen (2012) Stochastic non-smooth envelopment of data: Semi-parametric frontier estimation subject to shape constraints, *Journal of Productivity Analysis* 38(1), 11-28.
- Lee, C. Y., Johnson, A. L., Moreno-Centeno, E., & Kuosmanen, T. (2013). A more efficient algorithm for convex nonparametric least squares. *European Journal of Operational Research* 227(2): 391–400.
- Li, Q., and Racine, J. S. (2007). *Nonparametric econometrics: theory and practice*. Princeton University Press.
- Lim, E., and Glynn, P. W. (2012). Consistency of multidimensional convex regression. *Operations Research*, 60(1), 196-208.

- Mammen, E. (1991). Nonparametric regression under qualitative smoothness assumptions. *Annals of Statistics* 19, 741–59.
- Mazumder, R., Choudhury, A., Iyengar, G., & Sen, B. (2015). A Computational Framework for Multivariate Convex Regression and its Variants. *arXiv preprint arXiv:1509.08165*.
- Nesterov, Y. (2005). Smooth minimization of non-smooth functions. *Mathematical programming*, 103(1), 127-152.
- Pavcnik, N. (2002). Trade liberalization, exit, and productivity improvements: Evidence from Chilean plants. *The Review of Economic Studies*, 69(1), 245-276.
- Racine, J. S., and Li, Q. (2004). Nonparametric estimation of regression functions with both categorical and continuous data. *Journal of Econometrics* 119(1): 99–130.
- Robinson P.M. 1988. Root-N-consistent semiparametric regression. *Econometrica* 56:931-954.
- Sarath, B., Maindiratta, A. (1997). On the Consistency of Maximum Likelihood Estimation of Monotone and Concave Production Frontiers. *Journal of Productivity Analysis* 8(3): 239–246.
- Stone, C. J. (1977). Consistent Nonparametric Regression. *The Annals of Statistics*, 5(4), 595-620.
- Seijo, E., and B. Sen (2011). Nonparametric least squares estimation of a multivariate convex regression function. *Annals of Statistics* 39(3): 1633–1657.
- Varian, H. R. (1982). The nonparametric approach to demand analysis. *Econometrica: Journal of the Econometric Society*, 945-973.
- Varian, H.R. (1984). The nonparametric approach to production analysis. *Econometrica* 52(3):579-598.

Appendix A. Extensions to the CWB estimator and the relationship between SCKLS, CWB and CNLS

A.1. Calculating the first partial derivative of $\hat{g}(\mathbf{x}|p)$ for CWB

Du et al. (2013) proposed CWB estimator which requires estimating the first partial derivative of unconstrained functional estimates, $\hat{g}^{(1)}(\mathbf{x}|p)$ which are necessary to impose the constraints. Here, we tried two different methods to calculate the partial derivative. The first method is to calculate numerical derivative, $\hat{g}^{(1)}(\mathbf{x}|p) = \frac{\hat{g}(\mathbf{x} + \Delta|p) - \hat{g}(\mathbf{x}|p)}{\Delta}$, to obtain the approximated derivative as described by Du et al. The second method is to use the slope estimates of local linear estimator directly as a proxy for the first partial derivative. We evaluate the performance of CWB in p-space estimator with these two different methods. Table A1 and Table A2 summarize the RMSE on observed points and evaluation points respectively. The experimental setting is based on Experiment 1 in Section 5.1.

The results show that the CWB estimator using the numerical derivative performances much better than CWB using the slope estimates from the local linear kernel estimator particularly when the sample size is small, the difference in performance is large. A potential reason for this result is that the convergent rates of slope estimates in local linear estimator are slower than that of functional estimate. Thus, slope estimates are not very accurate when the dataset is small. In contrast, the numerical derivative uses the functional estimate to calculate the partial derivative of $\hat{g}(\mathbf{x}|p)$. Consequently, the numerical derivative does not suffer from the slow convergent rate of slope estimate of the local linear kernel.

Table A1. RMSE on observation points for different methods to obtain $\hat{g}^{(1)}(\mathbf{x}|p)$

Number of observations		Average RMSE on observation points				
		100	200	300	400	500
2-input	Numerical derivative	0.260	0.163	0.143	0.153	0.164
	Slope estimates of LL	0.421	0.357	0.284	0.306	0.293
3-input	Numerical derivative	0.236	0.256	0.208	0.246	0.240
	Slope estimates of LL	0.356	0.427	0.336	0.294	0.279
4-input	Numerical derivative	0.259	0.226	0.222	0.216	0.210
	Slope estimates of LL	0.388	0.397	0.276	0.261	0.259

Table A2. RMSE on evaluation points for different methods to obtain $\hat{g}^{(1)}(\mathbf{x}|p)$

Number of observations		Average RMSE on evaluation points				
		100	200	300	400	500
2-input	Numerical derivative	0.284	0.188	0.157	0.176	0.193
	Slope estimates of LL	0.445	0.387	0.321	0.334	0.323
3-input	Numerical derivative	0.309	0.355	0.272	0.331	0.271
	Slope estimates of LL	0.438	0.507	0.403	0.371	0.363
4-input	Numerical derivative	0.408	0.381	0.354	0.333	0.308
	Slope estimates of LL	0.530	0.535	0.396	0.387	0.368

A.2. CWB estimator that minimize the distance from the observed data

Since the objective function of CWB estimator potentially pulls the functional estimate away from the true function and towards the unrestricted estimate, CWB estimator may suffer from a finite sample bias. To avoid this problem, we propose an extension of CWB estimator by converting the objective function from p -space to y -space. Instead of minimizing the distance between the unconstrained estimator and the shape restricted functional estimate by minimizing the distance between the two functions in p -space, we propose minimizing the distance between the observed vector of y and the shape restricted functional estimate in y -space. The estimator is formulated as follows:

$$\begin{aligned}
\min_{\mathbf{p}} D_y(\mathbf{p}) &= \sum_{j=1}^n (y_j - \hat{g}(\mathbf{X}_j|\mathbf{p}))^2 \\
\text{subject to} & \\
l(\mathbf{x}_i) &\leq \hat{g}^{(s)}(\mathbf{x}_i|\mathbf{p}) \leq u(\mathbf{x}_i) \quad i = 1, \dots, m \\
\sum_{j=1}^n p_j &= 1
\end{aligned} \tag{A.1}$$

Since the objective function is not necessarily convex in \mathbf{p} , this problem is a general nonlinear optimization problem which is hard to solve. In appendix A.3, we show the relationship between our extension to CWB, which we will refer to as CWB in y-space, to Shape Constrained Kernel-weighted Least Squares (SCKLS), the estimator we propose in the following section.

A.3. The relationship between SCKLS, CWB and CNLS

We describe the relationship of CWB and SCKLS. To begin, note the concavity and monotonicity constraint in (6) are just examples of the more general constraints in either CWB in p-space (3) or in y-space. Comparing the objective function of CWB in y-space (A.1) and SCKLS (6), the SCKLS estimator is obtained by minimizing the weighted sum of squared residuals, while the CWB estimator in y-space is obtained by minimizing the sum of squared residuals. Namely, the kernel weight is used to weight the sum of squared residuals in the SCKLS estimator while it is used to weight each observation to obtain functional estimate $\hat{g}(\mathbf{X}_j|\mathbf{p})$ in the CWB estimator in y-space.

We also recognize that the CWB estimator in y-space has same sum of squared residuals objective functions. The only difference between them is the form of the functional and slope estimates as summarized in Table A3. The CNLS estimator defines the function and slope estimates as decision variables of the optimization problem. In contrast, the CWB estimator in y-space defines the function and slope estimates as consisting of two parts: the unrestricted local weighting estimator and observation

specific weights. This decomposition allows a smooth function to be estimated, but potentially leads to a non-convex objective function increasing the computational difficulty of the optimization problem. Further, this decomposition can introduce a finite sample bias because the estimate depends on the unrestricted local weighting estimates which are not necessarily close to the true function in the case of finite sample. Since we have already shown the relationship between SCKLS and CNLS in Section 4.2. , we also obtain indirectly the relationship between SCKLS and CWB estimator in y-space through CNLS estimator.

Table A3. Expression of functional and slope estimates

	CNLS	CWB in y-space
Functional estimates ($= \hat{g}(\mathbf{X}_j)$)	$\hat{y}_j = \hat{\alpha}_j + \hat{\beta}'_j \mathbf{X}_j$	$\sum_{l=1}^n \hat{p}_l \cdot A_l(\mathbf{X}_j) y_l$
Slope estimates ($= \frac{\partial \hat{g}}{\partial X}(\mathbf{X}_j)$)	$\hat{\beta}_j$	$\sum_{l=1}^n \hat{p}_l \cdot \frac{\partial A_l(\mathbf{X}_j)}{\partial X} y_l$

Appendix B. Comparison between piece-wise linear and smooth estimates

SCKLS estimator is piece-wise linear estimates which approximates a smooth true production function. Piece-wise linear functional estimators are often criticized as a rough approximation. In this section, we show that under monotonicity and concavity constraints, even smooth estimators tend to select approximately piece-wises linear estimates.

We estimate a production function using B-spline with monotonicity and concavity constraints. Recall B-splines is a smooth estimator which should not favor a piece-wise approximation. We impose the monotonicity and concavity on 50 uniform grid of evaluation points, and used 20 knots to estimate quadratic B-spline. We considered following DGP: Cobb-Douglas production function with one-input and one-output, $y = x^{0.5} + \epsilon$, where observed input x is randomly drawn from uniform distribution, $unif[1, 10]$, and noise, ϵ , is randomly sampled from a normal distribution, $N(0,0.5^2)$.

Figure A1 is the graph of the functional estimate of shape constrained B-spline. Although the both the true function and the estimator are smooth, visually the estimate appears to be a piece-wise linear function composed of three hyperplanes.

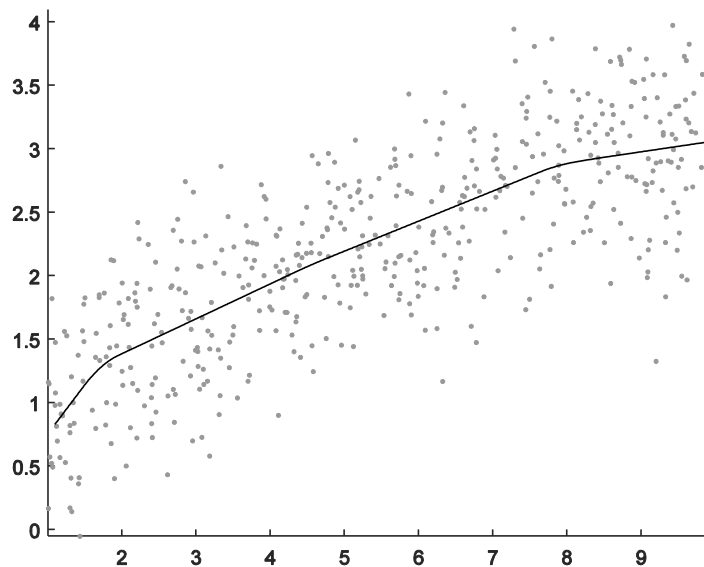


Figure A1. Functional estimates of Shape Constrained B-spline

Appendix C. An algorithm for SCKLS computational performance

For a given number of evaluation points, m , SCKLS requires $m(m - 1)$ concavity constraints. Larger values of m provide a more flexible functional estimate, but also increase the number of constraints quadratically, thus, the amount of time needed to solve one instance of the quadratic program increases quadratically. But note the analyst can select the number of evaluation points in SCKLS and CWB. By selecting m the computational complexity of can be potentially reduced relative to CNLS or estimates on denser grids, i.e. $m(m - 1) \ll n(n - 1)$.

Further, Dantzig et al. (1954, 1959) propose an iterative approach that reduces the size of large-

scale problems by relaxing a subset of the constraints and solving the relaxed model with only a subset V of constraints, checking which of the excluded constraints are violated, and iteratively adding violated constraints to the relaxed model until an optimal solution satisfies all constraints. Lee et al. (2013), who apply the approach to CNLS, find a significant reduction in computational time. Computational performances also improves if a subset of the constraints can be identified which are likely to be needed in the model. Lee et al. find the concavity constraints corresponding to pairs of observations that are close in terms of the L2 norm measure over input vectors and more likely to be binding than those corresponding to the distant observations. We use this insight to develop a strategy for identifying constraints to include in the initial subset V , when solving SCKLS as described below.

Given a grid to evaluate the constraints of the SCKLS estimator, we define the initial subset of constraints V as those constraints constructed by adjacent grid points as shown in Figure A2.

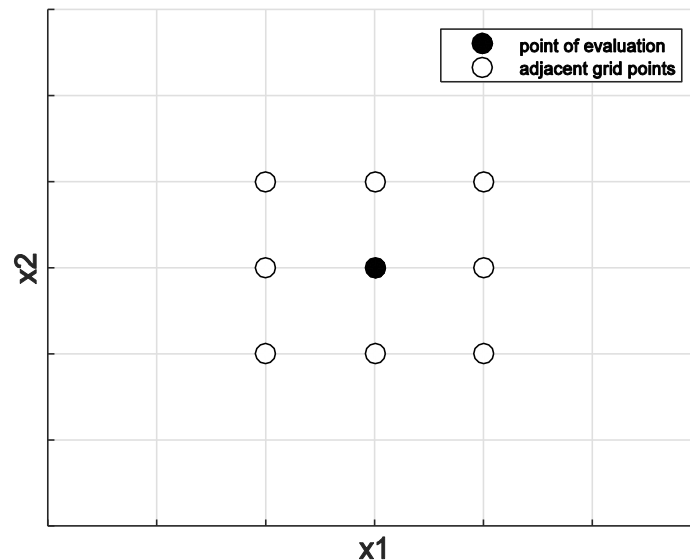


Figure A2. Definition of adjacent grid in two-dimensional case

Algorithm: Iterative approach for SCKLS computational speedup

- 1: $t \leftarrow 0$
 - 2: $V \leftarrow \{(i, l): \mathbf{x}_i \text{ and } \mathbf{x}_l \text{ are adjacent, } i < l\}$
 - 3: Solve relaxed SCKLS with V to find initial solution $\{a_i^{(0)}, \mathbf{b}_i^{(0)}\}_{i=1}^m$
 - 4: **while** $\{a_i^{(t)}, \mathbf{b}_i^{(t)}\}_{i=1}^m$ satisfies all constraints in (6) **do**
 - 5: $t \leftarrow t + 1$
 - 6: $U \leftarrow \{(i, l): \mathbf{x}_i \text{ and } \mathbf{x}_l \text{ do not satisfy constraints in (6)}\}$
 - 7: $V \leftarrow V \cup U$.
 - 8: Solve relaxed SCKLS with V to find solution $\{a_i^{(t)}, \mathbf{b}_i^{(t)}\}_{i=1}^m$
 - 9: **end while**
 - 10: **return** $\{a_i^{(t)}, \mathbf{b}_i^{(t)}\}_{i=1}^m$
-

Appendix D. Comprehensive results of Experiment 1

We compare following five estimators: SCKLS with fixed bandwidth, SCKLS with variable bandwidth, CNLS, CWB in p-space and CWB in y-space, Local Linear Kernel, and parametric Cobb-Douglas function estimated via ordinary least squares (OLS). Table A4 and Table A5 show the RMSE of Experiment 1 on observation points and evaluation points respectively.

Table A4. RMSE on observation points for Experiment 1

Number of observations		Average of RMSE on observation points				
		100	200	300	400	500
2-input	SCKLS fixed bandwidth	0.193	0.171	0.141	0.132	0.118
	SCKLS variable bandwidth	0.183	0.158	0.116	0.118	0.098
	CNLS	0.229	0.163	0.137	0.138	0.116
	CWB in p-space	0.189	0.167	0.158	0.140	0.129
	CWB in y-space	0.205	0.136	0.173	0.141	0.120
	Local Linear	0.212	0.166	0.149	0.152	0.140
	Cobb-Douglas	0.078	0.075	0.048	0.039	0.043
3-input	SCKLS fixed bandwidth	0.230	0.187	0.183	0.152	0.165
	SCKLS variable bandwidth	0.216	0.183	0.175	0.143	0.142
	CNLS	0.294	0.202	0.189	0.173	0.168
	CWB in p-space	0.228	0.221	0.210	0.183	0.172
	CWB in y-space	0.209	0.362	0.218	0.154	0.160
	Local Linear	0.250	0.230	0.235	0.203	0.181
	Cobb-Douglas	0.104	0.089	0.070	0.047	0.041
4-input	SCKLS fixed bandwidth	0.225	0.248	0.228	0.203	0.198
	SCKLS variable bandwidth	0.217	0.219	0.210	0.180	0.179
	CNLS	0.315	0.294	0.246	0.235	0.214
	CWB in p-space	0.238	0.262	0.231	0.234	0.198
	CWB in y-space	0.222	0.240	0.248	0.303	0.332
	Local Linear	0.256	0.297	0.252	0.240	0.226
	Cobb-Douglas	0.120	0.073	0.091	0.067	0.063

Table A5. RMSE on evaluation points for Experiment 1

Number of observations		Average of RMSE on evaluation points				
		100	200	300	400	500
2-input	SCKLS fixed bandwidth	0.219	0.189	0.150	0.147	0.128
	SCKLS variable bandwidth	0.212	0.176	0.125	0.132	0.103
	CNLS	0.350	0.299	0.260	0.284	0.265
	CWB in p-space	0.206	0.186	0.174	0.154	0.143
	CWB in y-space	0.259	0.228	0.228	0.172	0.167
	Local Linear	0.247	0.182	0.167	0.171	0.156
	Cobb-Douglas	0.076	0.076	0.049	0.040	0.043
3-input	SCKLS fixed bandwidth	0.283	0.231	0.238	0.213	0.215
	SCKLS variable bandwidth	0.292	0.237	0.235	0.196	0.187
	CNLS	0.529	0.587	0.540	0.589	0.598
	CWB in p-space	0.291	0.289	0.269	0.252	0.233
	CWB in y-space	0.314	0.474	0.265	0.346	0.261
	Local Linear	0.336	0.340	0.360	0.326	0.264
	Cobb-Douglas	0.116	0.098	0.080	0.052	0.046
4-input	SCKLS fixed bandwidth	0.321	0.357	0.329	0.308	0.290
	SCKLS variable bandwidth	0.378	0.348	0.363	0.320	0.301
	CNLS	0.845	0.873	0.901	0.827	0.792
	CWB in p-space	0.360	0.385	0.358	0.361	0.325
	CWB in y-space	0.355	0.470	0.338	0.410	0.602
	Local Linear	0.482	0.527	0.483	0.495	0.445
	Cobb-Douglas	0.146	0.091	0.115	0.081	0.080

Table A6 shows the computational time of Experiment 1 for each estimator.

Table A6. Computational time for Experiment 1

Number of observations	Average of computational time in seconds; (percentage of Afriat constraints included in the final optimization problem)					
	100	200	300	400	500	
2-input	SCKLS fixed bandwidth	14.1 (6.14%)	13.3 (5.28%)	42.2 (8.86%)	34.7 (7.80%)	77.4 (8.31%)
	SCKLS variable bandwidth	16.4 (3.47%)	33.9 (3.44%)	27.6 (3.34%)	36.0 (3.22%)	50.6 (3.53%)
	CNLS	2.0 (100%)	6.1 (100%)	16.5 (100%)	26.5 (100%)	55.3 (100%)
	CWB in p-space	24.1 (2.39%)	33.2 (2.35%)	76.6 (2.35%)	82.3 (2.35%)	130 (2.35%)
	CWB in y-space	39.3 (2.35%)	92.7 (2.35%)	111 (2.35%)	190 (2.35%)	233 (2.36%)
	SCKLS fixed bandwidth	26.9 (16.0%)	40.4 (16.6%)	45.5 (16.3%)	67.3 (16.4%)	136 (16.2%)
3-input	SCKLS variable bandwidth	20.0 (15.7%)	42.0 (15.9%)	37.4 (15.8%)	47.1 (15.8%)	58.2 (15.9%)
	CNLS	3.8 (100%)	16.4 (100%)	37.0 (100%)	82.9 (100%)	161 (100%)
	CWB in p-space	47.6 (15.5%)	71.5 (15.5%)	100 (15.5%)	202 (15.5%)	255 (15.5%)
	CWB in y-space	120 (15.5%)	357 (15.5%)	443 (15.5%)	529 (15.5%)	424 (15.5%)
	SCKLS fixed bandwidth	47.5 (40.1%)	71.6 (39.9%)	77.4 (39.9%)	166 (40.0%)	235 (39.8%)
	SCKLS variable bandwidth	26.8 (39.9%)	45.6 (40.0%)	46.8 (39.8%)	60.5 (39.9%)	74.8 (39.8%)
4-input	CNLS	5.8 (100%)	22.4 (100%)	79.1 (100%)	139.8 (100%)	287.8 (100%)
	CWB in p-space	68.8 (39.8%)	136 (39.8%)	196 (39.8%)	327 (39.8%)	442 (39.8%)
	CWB in y-space	91.3 (39.8%)	175 (39.8%)	195 (39.8%)	535 (39.8%)	545 (39.8%)
	SCKLS fixed bandwidth	47.5 (40.1%)	71.6 (39.9%)	77.4 (39.9%)	166 (40.0%)	235 (39.8%)

Appendix E. Comprehensive results of Experiment 2

We compare following five estimators: SCKLS with fixed bandwidth, SCKLS with variable bandwidth, CNLS, CWB in p-space, CWB in y-space, Local Linear Kernel, and parametric Cobb-Douglas function estimated via ordinary least squares (OLS). Table A7 and Table A8 show the RMSE of Experiment 2 on observation points and evaluation points respectively.

Table A7. RMSE on observation points for Experiment 2

Number of observations		Average of RMSE on observation points				
		100	200	300	400	500
2-input	SCKLS fixed bandwidth	0.239	0.203	0.203	0.155	0.140
	SCKLS variable bandwidth	0.240	0.185	0.168	0.139	0.119
	CNLS	0.279	0.231	0.194	0.168	0.151
	CWB in p-space	0.314	0.215	0.237	0.275	0.151
	CWB in y-space	0.241	0.229	0.173	0.178	0.206
	Local Linear	0.287	0.244	0.230	0.214	0.161
	Cobb-Douglas	0.109	0.108	0.081	0.042	0.048
3-input	SCKLS fixed bandwidth	0.292	0.263	0.221	0.204	0.184
	SCKLS variable bandwidth	0.281	0.242	0.198	0.180	0.175
	CNLS	0.379	0.303	0.275	0.224	0.214
	CWB in p-space	0.318	0.306	0.308	0.244	0.214
	CWB in y-space	0.281	0.273	0.225	0.320	0.271
	Local Linear	0.333	0.306	0.288	0.259	0.214
	Cobb-Douglas	0.176	0.118	0.101	0.084	0.072
4-input	SCKLS fixed bandwidth	0.317	0.291	0.249	0.241	0.254
	SCKLS variable bandwidth	0.290	0.254	0.236	0.222	0.215
	CNLS	0.491	0.356	0.311	0.293	0.313
	CWB in p-space	0.400	0.318	0.273	0.260	0.289
	CWB in y-space	0.312	0.338	0.262	0.365	0.453
	Local Linear	0.335	0.342	0.257	0.274	0.283
	Cobb-Douglas	0.157	0.150	0.112	0.075	0.077

Table A8. RMSE on evaluation points for Experiment 2

Number of observations		Average of RMSE on evaluation points				
		100	200	300	400	500
2-input	SCKLS fixed bandwidth	0.253	0.225	0.222	0.172	0.160
	SCKLS variable bandwidth	0.255	0.205	0.179	0.149	0.135
	CNLS	0.319	0.355	0.334	0.255	0.267
	CWB in p-space	0.329	0.239	0.262	0.305	0.177
	CWB in y-space	0.263	0.241	0.198	0.228	0.180
	Local Linear	0.330	0.272	0.257	0.239	0.194
	Cobb-Douglas	0.112	0.112	0.083	0.044	0.049
3-input	SCKLS fixed bandwidth	0.367	0.339	0.302	0.268	0.231
	SCKLS variable bandwidth	0.364	0.303	0.256	0.230	0.224
	CNLS	0.743	0.778	0.744	0.696	0.620
	CWB in p-space	0.398	0.392	0.434	0.336	0.274
	CWB in y-space	0.401	0.473	0.385	0.450	0.525
	Local Linear	0.452	0.444	0.438	0.398	0.302
	Cobb-Douglas	0.202	0.130	0.110	0.093	0.079
4-input	SCKLS fixed bandwidth	0.405	0.460	0.349	0.350	0.347
	SCKLS variable bandwidth	0.419	0.434	0.375	0.354	0.315
	CNLS	1.019	0.950	0.985	1.043	1.106
	CWB in p-space	0.514	0.520	0.393	0.390	0.452
	CWB in y-space	0.514	0.513	0.425	0.501	0.708
	Local Linear	0.524	0.626	0.451	0.491	0.550
	Cobb-Douglas	0.187	0.194	0.134	0.092	0.091

Appendix F. Comprehensive results of Experiment 3

We compare following four estimators: SCKLS with fixed bandwidth, SCKLS with variable bandwidth, CNLS, CWB in p-space with uniform/non-uniform grid. Table A9 and Table A10 show the RMSE of Experiment 3 on observation points and evaluation points respectively.

Table A9. RMSE on observation points for Experiment 3

Number of observations		Average of RMSE on observation points				
		100	200	300	400	500
2-input	SCKLS fixed/uniform	0.179	0.151	0.144	0.121	0.108
	SCKLS fixed/non-uniform	0.185	0.153	0.159	0.123	0.107
	SCKLS variable/uniform	0.183	0.156	0.142	0.125	0.104
	SCKLS variable/non-uniform	0.176	0.144	0.132	0.114	0.093
	CNLS	0.193	0.160	0.140	0.130	0.117
	CWB p-space/uniform	0.256	0.162	0.180	0.139	0.125
	CWB p-space/non-uniform	0.243	0.160	0.174	0.135	0.125
3-input	SCKLS fixed/uniform	0.197	0.184	0.172	0.164	0.167
	SCKLS fixed/non-uniform	0.200	0.181	0.173	0.161	0.172
	SCKLS variable/uniform	0.212	0.187	0.170	0.175	0.170
	SCKLS variable/non-uniform	0.210	0.180	0.162	0.160	0.155
	CNLS	0.303	0.246	0.201	0.185	0.166
	CWB p-space/uniform	0.243	0.436	0.173	0.174	0.184
	CWB p-space/non-uniform	0.233	0.194	0.176	0.165	0.173
4-input	SCKLS fixed/uniform	0.219	0.211	0.196	0.209	0.187
	SCKLS fixed/non-uniform	0.210	0.206	0.181	0.197	0.180
	SCKLS variable/uniform	0.208	0.193	0.167	0.171	0.170
	SCKLS variable/non-uniform	0.206	0.193	0.164	0.169	0.168
	CNLS	0.347	0.292	0.250	0.228	0.218
	CWB p-space/uniform	0.219	0.205	0.205	0.184	0.218
	CWB p-space/non-uniform	0.221	0.205	0.182	0.170	0.170

Table A10. RMSE on evaluation points for Experiment 3

	Number of observations	Average of RMSE on evaluation points				
		100	200	300	400	500
2-input	SCKLS fixed/uniform	0.262	0.220	0.244	0.157	0.196
	SCKLS fixed/non-uniform	0.212	0.174	0.195	0.138	0.131
	SCKLS variable/uniform	0.246	0.204	0.192	0.142	0.136
	SCKLS variable/non-uniform	0.193	0.160	0.145	0.120	0.100
	CNLS	0.435	0.402	0.404	0.379	0.381
	CWB p-space/uniform	0.422	0.287	0.376	0.246	0.264
	CWB p-space/non-uniform	0.283	0.186	0.215	0.159	0.162
3-input	SCKLS fixed/uniform	0.323	0.308	0.311	0.286	0.293
	SCKLS fixed/non-uniform	0.268	0.254	0.259	0.235	0.249
	SCKLS variable/uniform	0.335	0.303	0.281	0.262	0.254
	SCKLS variable/non-uniform	0.278	0.243	0.219	0.212	0.196
	CNLS	0.828	0.824	0.828	0.786	0.782
	CWB p-space/uniform	0.438	0.684	0.357	0.363	0.350
	CWB p-space/non-uniform	0.315	0.265	0.257	0.235	0.242
4-input	SCKLS fixed/uniform	0.406	0.398	0.397	0.404	0.400
	SCKLS fixed/non-uniform	0.339	0.343	0.333	0.371	0.331
	SCKLS variable/uniform	0.417	0.423	0.368	0.364	0.356
	SCKLS variable/non-uniform	0.359	0.359	0.313	0.302	0.280
	CNLS	1.129	1.107	1.220	1.196	1.223
	CWB p-space/uniform	0.421	0.442	0.435	0.418	0.487
	CWB p-space/non-uniform	0.354	0.344	0.308	0.286	0.280

Appendix G. Comprehensive results of Experiment 4

We compare following four estimators: SCKLS with fixed bandwidth, SCKLS with variable bandwidth, CWB in p-space and CWB in y-space. Table A11 and Table A12 show the RMSE of Experiment 4 on observation points and evaluation points respectively.

Table A11. RMSE on observation points for Experiment 4

Number of evaluation points		Average of RMSE on observation points		
		100	300	500
2-input	SCKLS fixed bandwidth	0.142	0.141	0.141
	SCKLS variable bandwidth	0.113	0.112	0.112
	CWB in p-space	0.149	0.151	0.156
	CWB in y-space	0.225	0.122	0.129
3-input	SCKLS fixed bandwidth	0.198	0.203	0.197
	SCKLS variable bandwidth	0.169	0.167	0.166
	CWB in p-space	0.218	0.234	0.231
	CWB in y-space	0.345	0.241	0.222
4-input	SCKLS fixed bandwidth	0.239	0.207	0.206
	SCKLS variable bandwidth	0.195	0.192	0.191
	CWB in p-space	0.219	0.227	0.296
	CWB in y-space	0.466	0.290	0.292

Table A12. RMSE on evaluation points for Experiment 4

Number of evaluation points		Average of RMSE on evaluation points		
		100	200	300
2-input	SCKLS fixed bandwidth	0.181	0.164	0.158
	SCKLS variable bandwidth	0.140	0.128	0.124
	CWB in p-space	0.195	0.180	0.179
	CWB in y-space	0.262	0.162	0.169
3-input	SCKLS fixed bandwidth	0.304	0.267	0.257
	SCKLS variable bandwidth	0.242	0.213	0.205
	CWB in p-space	0.332	0.329	0.302
	CWB in y-space	0.792	0.582	0.559
4-input	SCKLS fixed bandwidth	0.383	0.296	0.270
	SCKLS variable bandwidth	0.386	0.304	0.265
	CWB in p-space	0.403	0.359	0.415
	CWB in y-space	1.040	0.352	0.381

Table A13 shows the computational time of Experiment 4 for each estimator.

Table A13. Computational time for Experiment 4

Number of evaluation points	Average of computational time in seconds; (percentage of Afriat constraints included in the final optimization problem)			
	100	300	500	
2-input	SCKLS fixed bandwidth	26.6 (11.7%)	28.3 (6.56%)	34.0 (5.45%)
	SCKLS variable bandwidth	21.3 (9.90%)	21.6 (4.41%)	24.9 (3.19%)
	CWB in p-space	41.0 (8.77%)	56.5 (3.21%)	74.2 (1.95%)
	CWB in y-space	52.8 (8.76%)	103 (3.21%)	146 (1.95%)
3-input	SCKLS fixed bandwidth	84.8 (29.1%)	112 (16.7%)	134 (13.3%)
	SCKLS variable bandwidth	21.1 (28.5%)	37.2 (15.8%)	59.1 (12.4%)
	CWB in p-space	121 (28.2%)	221 (15.5%)	310 (12.2%)
	CWB in y-space	181 (28.2%)	625 (15.5%)	948 (12.2%)
4-input	SCKLS fixed bandwidth	149 (62.3%)	170 (40.0%)	597 (27.7%)
	SCKLS variable bandwidth	24.6 (62.1%)	52.7 (39.9%)	468 (27.5%)
	CWB in p-space	175 (61.9%)	275 (39.8%)	729 (27.4%)
	CWB in y-space	189 (61.9%)	288 (39.8%)	579 (27.4%)

Appendix H. Semiparametric partially linear model to integrate contextual variable

We integrate semiparametric partially linear model into SCKLS estimator to consider contextual variables. The partially linear model is one of the simplest semiparametric models often used in practice. The model of SCKLS estimator with contextual variables is represented as follows:

$$y_j = \mathbf{Z}_j' \boldsymbol{\gamma} + g(\mathbf{X}_j) + \epsilon_j \quad (\text{A.2})$$

where $\mathbf{Z}_j = (Z_{j1}, Z_{j2}, \dots, Z_{jk})'$ denotes contextual variables and $\boldsymbol{\gamma} = (\gamma_1, \gamma_2, \dots, \gamma_k)'$ is the coefficient of contextual variables, Johnson and Kuosmanen (2011, 2012). Then, we estimate the coefficient of contextual variable at the first step:

$$\hat{\boldsymbol{\gamma}} = \left(\sum_{j=1}^n \tilde{\mathbf{Z}}_j \tilde{\mathbf{Z}}_j' \right)^{-1} \left(\sum_{j=1}^n \tilde{\mathbf{Z}}_j \tilde{y}_j \right) \quad (\text{A.3})$$

where $\tilde{\mathbf{Z}}_j = \mathbf{Z}_j - \hat{E}[\mathbf{Z}_j | \mathbf{X}_j]$ and $\tilde{y}_j = y_j - \hat{E}[y_j | \mathbf{X}_j]$ respectively, and each conditional expectation is estimated by kernel estimation method such as local linear. Finally, we apply the SCKLS estimator to the data $\{\mathbf{X}_j, y_j - \mathbf{Z}_j \hat{\boldsymbol{\gamma}}\}_{j=1}^n$. For details of partially linear model, see Li and Racine (2007).

References

- Dantzig, G.B., Fulkerson, D.R., Johnson, S.M., 1954. Solution of a large-scale traveling salesman problem. *Operations Research* 2: 393–410.
- Dantzig, G.B., Fulkerson, D.R., Johnson, S.M., 1959. On a linear-programming combinatorial approach to the traveling-salesman problem. *Operations Research* 7: 58–66.
- Du, P., Parmeter, C.F., Racine, J.S. (2013). Nonparametric kernel regression with multiple predictors and multiple shape constraints. *Statistica Sinica* 23(3): 1347–1371.
- Johnson, A.L. and T. Kuosmanen, 2011. One-stage estimation of the effects of operational conditions and practices on productive performance: Asymptotically normal and efficient, root-n consistent StoNEZD method. *Journal of Productivity Analysis* 36(2): 219-230.
- Johnson, A.L. and T. Kuosmanen, 2012. One-stage and Two-stage DEA Estimation of the Effects of Contextual Variables. *European Journal of Operational Research* 220(2): 559-570.